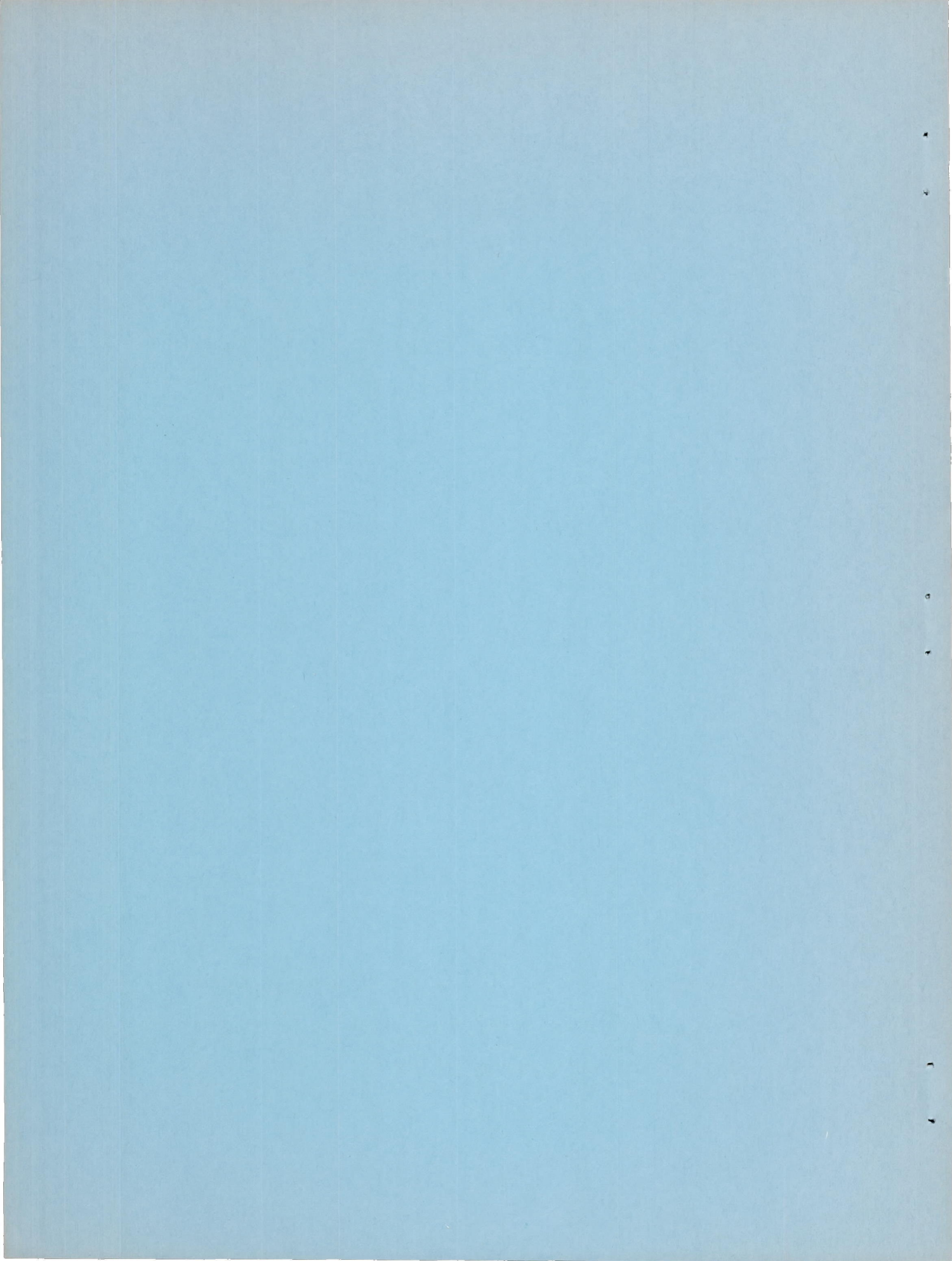# NACA

RESEARCH MEMORANDUM

AN INVESTIGATION THROUGHOUT THE SUBSONIC SPEED RANGE OF

A FULL-SPAN AND A SEMISPAN MODEL OF A PLANE WING

AND OF A CAMBERED AND TWISTED WING, ALL

HAVING 45° OF SWEEPBACK

By Harry H. Shibata, Angelo Bandettini,
and Joseph Cleary

Ames Aeronautical Laboratory
Moffett Field, Calif.

NATIONAL ADVISORY COMMITTEE
FOR AERONAUTICS

WASHINGTON

June 26, 1952
Declassified April 6, 1956

NATIONAL ADVISORY COMMITTEE FOR AERONAUTICS

RESEARCH MEMORANDUM

AN INVESTIGATION THROUGHOUT THE SUBSONIC SPEED RANGE OF

A FULL-SPAN AND A SEMISPAN MODEL OF A PLANE WING

AND OF A CAMBERED AND TWISTED WING, ALL

HAVING 45° OF SWEEPBACK

By Harry H. Shibata, Angelo Bandettini,
and Joseph Cleary

SUMMARY

A wind-tunnel investigation has been made of two full-span and two semispan models having 45° of sweepback, an aspect ratio of 5.5, and a taper ratio of 0.53. One wing had no camber and twist and the other wing was cambered for a design lift coefficient of 0.4 and twisted to relieve the loading at the tip which accompanies sweepback. The airfoil sections normal to the quarter-chord line were the NACA 64A010 for the plane wing and the NACA 64A810 for the cambered and twisted wing. The cambered and twisted wing had 9.37° of washout between the root and the tip. The tests were made at Mach numbers from 0.25 to 0.92. At a Mach number of 0.25, the maximum Reynolds number was 10,000,000. The full-span models were also tested at Reynolds numbers varying from 1,000,000 at 0.60 Mach number to 4,900,000 at a Mach number of 0.92. In addition, the effects of one particular type of surface roughness were investigated on both wings.

The lift and drag data obtained from tests of the semispan model agreed well with data obtained on the full-span model. In general, the aerodynamic center of the semispan model was slightly rearward of its position on the full-span model.

The results obtained from tests of the full-span models at a Reynolds number of 2,000,000 and Mach numbers from 0.25 to 0.92 agree well with the previously reported results of tests of semispan models employing similar wings. Increasing the Reynolds number over the Mach number range had only a small effect on the characteristics of the plane wing. The data indicate the cambered and twisted wing was more sensitive

to changes in Reynolds number over the Mach number range than the plane wing. Increasing the Reynolds number at the higher Mach numbers resulted in an increase in the lift coefficient at which static instability first occurred.

The addition of a particular type of surface roughness did not have a significant effect on the aerodynamic characteristics of the plane wing. However, for the cambered and twisted wing, at Mach numbers of 0.80 and above, this type of roughness resulted in a more linear variation of lift coefficient with angle of attack and increased the drag at moderate lift coefficients. At Mach numbers of 0.80 and above, the lift coefficient at which the wing became unstable was reduced by the addition of roughness.

INTRODUCTION

Theoretical studies and a number of experimental investigations have indicated that camber and twist will improve the characteristics of swept wings. This improvement results from more uniform distribution of load, both spanwise and chordwise, which alleviates the flow separation and the attendant stability deterioration and drag increase at moderate and high lift coefficients. References 1 and 2 have demonstrated that camber and twist can improve the characteristics of swept wings at low speeds, and reference 3 shows the effects of camber and twist at Mach numbers up to 0.94.

The data of references 1, 2, and 3 were obtained by use of semispan models mounted vertically on the tunnel test-section floor. Flow separation on wings may be influenced by the tunnel-floor boundary layer. Such an effect was noted in references 4 and 5 during tests of wing-alone models. Use of a semifuselage in combination with a semispan wing, as was done in the tests reported in references 1, 2, and 3, may be expected to minimize these effects. The possibility still exists that with semispan wing-fuselage combinations, the influence of the tunnel-floor boundary layer may alter the flow over the wings to such an extent as to make questionable any conclusions regarding the effects of camber and twist. It was therefore deemed desirable to obtain comparative data on both semispan and full-span models of plane wings and cambered and twisted wings to determine the validity of the conclusions reached on the basis of previous investigations of semispan models.

For this reason, an investigation has been conducted in the Ames 12-foot pressure tunnel at Mach numbers up to 0.92 of two 45° swept-back, sting-mounted, wing-fuselage models, one having a cambered and twisted wing and the other a plane wing, and of two semispan wing-fuselage combinations, identical in every respect to the full-span models. To

extend the study of camber and twist to include the effects of higher Reynolds numbers at high subsonic speeds, the two full-span models were also tested in the Ames 16-foot high-speed wind tunnel.

COEFFICIENTS AND SYMBOLS

The following coefficients and symbols are used in this report:

b wing span measured perpendicular to the plane of symmetry, feet

c local chord measured parallel to plane of symmetry, feet

c' local chord measured perpendicular to the quarter-chord line, feet

$\bar{c}$ wing mean aerodynamic chord $\left(\dfrac{\int_0^{b/2} c^2 \, dy}{\int_0^{b/2} c \, dy} \right)$, feet

C_D drag coefficient $\left(\dfrac{\text{drag}}{qS} \right)$

$C_{D_{min}}$ minimum drag coefficient

C_L lift coefficient $\left(\dfrac{\text{lift}}{qS} \right)$

C_m pitching-moment coefficient about the lateral axis through the quarter point of the wing mean aerodynamic chord $\left(\dfrac{\text{pitching moment}}{qS\bar{c}} \right)$

$\left(\dfrac{L}{D} \right)_{max}$ maximum lift-drag ratio

l length of body including portion removed to accommodate sting, feet

M Mach number $\left(\dfrac{V}{\text{speed of sound}}\right)$

q dynamic pressure $\left(\dfrac{1}{2}\rho V^2\right)$, pounds per square foot

R Reynolds number $\left(\dfrac{\rho V \bar{c}}{\mu}\right)$

r radius of body, feet

r_o maximum radius of body, feet

S area of model wing, square feet

V free-stream velocity, feet per second

x longitudinal distance, feet

y lateral distance, feet

α angle of attack of the body longitudinal axis, degrees

α_t angle of twist with reference to root chord (positive for washin), degrees

ρ mass density of air, slugs per cubic foot

μ coefficient of viscosity of air, slugs per foot-second

C_{L_α} $\left(\dfrac{\partial C_L}{\partial \alpha}\right)$ (measured at $C_L = 0$), per degree

$C_{m_{C_L}}$ $\left(\dfrac{\partial C_m}{\partial C_L}\right)$ (measured at $C_L = 0$)

MODELS AND APPARATUS

A sketch of the full-span models is shown in figure 1(a) and a sketch of the semispan models in figure 1(b).

The wing models used in this investigation were of similar plan form and represented wings having an aspect ratio of 5.50, a taper ratio of 0.53, and a sweepback of the quarter-chord line of 45°. The profile of the uncambered, untwisted wing, hereinafter referred to as the plane wing, was the NACA 64A010 in planes normal to the quarter-chord line. The profile of the wing, hereinafter referred to as the cambered and twisted wing, was the NACA 64A810 with a modified $a = 0.8$ mean line (reference 6), in planes normal to the quarter-chord line. The angle of twist of the cambered and twisted wing varied from 0° at the root to -9.37° (washout) at the tip as shown in figure 1(a). This twist distribution was a straight-line-element type wherein all constant-percent points of the local chord lie in straight lines along the span. As a result of maintaining the local chords of the root and tip constant while the wing was twisted, the projected area of the cambered and twisted wing was approximately 0.5 percent less than that of the plane wing. In the reduction of all force and moment data to aerodynamic coefficients, this difference in wing areas was neglected and the area and the mean aerodynamic chord of the plane wing were used.

The body used for both the full-span and semispan models had a fineness ratio of 12.5, assuming closure at the tail as indicated by the dashed lines in figure 1. The after 19 percent of the body length of the full-span model was cut off to permit installation on the sting support. The after 19 percent of the semispan model body was also cut off in order to duplicate better the flow conditions at the rear of the full-span model body. Orifices were provided in the after end of the semispan model body to measure the base pressure. The plane wing was mounted with its root chord coincident with the longitudinal axis of the body. The cambered and twisted wing was centrally mounted but with -0.63° incidence of the root chord relative to the longitudinal axis of the body.

The majority of tests were conducted in the Ames 12-foot pressure wind tunnel, which is a closed-throat, variable-density wind tunnel with a low turbulence level closely approximating that of free air. Additional tests of the full-span models were conducted in the Ames 16-foot high-speed wind tunnel, which is a closed-throat wind tunnel having a stagnation pressure approximately equal to atmospheric pressure. The sting-supported, full-span model was mounted centrally in both the 12-foot and the 16-foot wind tunnels.

Figure 2(a) shows the full-span model mounted in the Ames 12-foot pressure wind tunnel. The diameter of the sting supporting the model was 83 percent of the diameter of the body base in both wind tunnels. All forces and moments were measured by means of a 4-inch-diameter, four-component, strain-gage balance of the type described in reference 7. This balance was mounted on the sting support and enclosed within the body of the model.

The semispan model, figure 2(b), was mounted with the wing perpendicular to the floor which served as a reflection plane. The gap between the body and the tunnel floor was approximately one-eighth inch.

Surface roughness was produced on the wing of the full-span model by the addition of a 1/8-inch-wide strip of number 60 carborundum centered on the 10-percent chord line on both upper and lower surfaces.

TESTS

Lift, drag, and pitching-moment data were obtained in the Ames 12-foot pressure wind tunnel for the plane wing and the cambered and twisted wing, each of which was tested full span on the sting support and semispan on the tunnel floor.

Additional tests were conducted in the Ames 16-foot high-speed wind tunnel to investigate the effect on the full-span model of higher Reynolds numbers at various Mach numbers. Tests in the 16-foot wind tunnel were also conducted to obtain the effects of surface roughness. The range of Reynolds numbers and Mach numbers at which tests were conducted is shown in figure 3.

For the tests in the Ames 12-foot pressure wind tunnel at the lower Mach numbers and Reynolds numbers, the angle of attack of the full-span model was varied from -4° to $+24^\circ$ and the angle of attack of the semispan model was varied from -6° to $+26^\circ$. The angle-of-attack range for the full-span models was reduced at the higher Mach numbers and Reynolds numbers where wind-tunnel power limitations, balance load limitations, or model vibration prevented testing at the higher angles. The angle-of-attack range for the semispan models was reduced at the higher Mach numbers where wind-tunnel power limitations prevented testing at the higher angles.

The angle-of-attack range of the full-span models tested in the Ames 16-foot high-speed wind tunnel was from -0.7° to 24° at the low Mach numbers and was limited to smaller angles at the higher Mach numbers by wind-tunnel power limitations and model vibration.

CORRECTIONS TO DATA

Corrections have been applied to the data of both full-span and semispan models to account for the effects of tunnel-wall interference, constriction due to the tunnel walls, base pressure, and tare forces.

Tunnel-Wall Interference

Corrections for tunnel-wall interference resulting from lift on the models were computed using the method of references 8 and 9 for the full-span and semispan models in the 12-foot wind tunnel and the method of reference 8 for the full-span model in the 16-foot wind tunnel. The following corrections were added:

	Full-span model		Semispan model
	12-ft wind tunnel	16-ft wind tunnel	12-ft wind tunnel
$\Delta\alpha$	$0.513\ c_L$	$0.434\ c_L$	$0.271\ c_L$
Δc_D	$0.00896\ c_L{}^2$	$0.00758\ c_L{}^2$	$0.00430\ c_L{}^2$
Δc_m	0	0	0

Constriction Effects

Corrections to the data to account for the constriction effects of the tunnel walls have been evaluated by the method of reference 10. The magnitudes of the corrections as applied to Mach number and dynamic pressure are illustrated by the following table:

Corrected Mach number	Uncorrected Mach number			$\dfrac{q_{corrected}}{q_{uncorrected}}$		
	Full-span model		Semispan model	Full-span model		Semispan model
	12-foot wind tunnel	16-foot wind tunnel	12-foot wind tunnel	12-foot wind tunnel	16-foot wind tunnel	12-foot wind tunnel
0.250	0.250	0.250	0.250	1.003	1.001	1.001
.600	.599	.599	.599	1.004	1.002	1.002
.800	.795	.797	.797	1.008	1.004	1.004
.850	.843	.845	.846	1.010	1.005	1.005
.900	.887	.892	.893	1.015	1.008	1.008
.920	.904	.909	.911	1.018	1.011	1.010

Base-Pressure Corrections

In an effort to correct at least partially for the interference of the sting support on the body of the full-span models, the base pressure was measured and the drag data were corrected to correspond to a base pressure equal to the static pressure of the free stream.

Base pressures were also measured on the semispan models and similar drag corrections were made in an effort to obtain comparable full-span and semispan model data.

Tares

Full-span model.- There were no tares due to direct air forces on the model-support equipment. Corrections were applied to account for static tares due to the weight of the model and to the variation of model attitude throughout the angle-of-attack range.

Semispan model.- Tare corrections due to the air forces exerted on the turntable were measured with the model removed from the tunnel. Possible interference effects between the model and the turntable were not evaluated. No attempt was made to remove the tunnel-floor boundary layer which, at the location of the model, had a displacement thickness of approximately 0.5 inch. The boundary-layer displacement thickness over the body in the region of the wing was approximately 0.15 inch. The tare drag coefficients subtracted from the data, representing the drag coefficients of the exposed surface of the turntable expressed in terms of wing area, are presented in the following table:

Reynolds number	Mach number				
	0.25	0.80	0.85	0.90	0.92
2,000,000	0.0050	0.0057	0.0060	0.0065	0.0068
6,000,000	.0049	- - -	- - -	- - -	- - -
10,000,000	.0049	- - -	- - -	- - -	- - -

RESULTS

The results of this investigation are presented in the figures indicated in the following outline:

DISCUSSION

Comparison of the Data for the Full-Span and Semispan Models

Inspection of the full-span and semispan model data at the same
Reynolds numbers and Mach numbers (figs. 4 through 15) indicates only
small effect due to the type of model support. In general, the lift
curves were nearly identical, the drag at low values of lift coefficient
was slightly larger for the semispan models, and the semispan models
had slightly greater static stability at low lift coefficients. Both
the plane wing and the cambered and twisted wing exhibited instability
at the higher lift coefficients. The lift coefficient at which this
instability occurred was little affected by the type of model support,
but the semispan model generally had a more rearward position of the
center of pressure at this lift coefficient than did the full-span
model. These differences were little affected by changes of either
Mach number or Reynolds number.

On the basis of available data, it is believed that the effects of
the type of model support on the pitching moment can be largely attri-
buted to the loss of lift near the root of the semispan model wing
caused by the interference between the model and the reflection-plane
boundary layer as noted in references 4 and 5.

Other factors which could affect the results of the full-span and
semispan tests include an insufficient correction for the type of model
support (sting and turntable interference) and the location of the model
in the air stream of the test section (tunnel-wall interference). These
effects are believed to be small in comparison to the reflection-plane
boundary-layer effect mentioned previously.

Full-Span Model Data

All of the data for the full-span models presented in figures 16
through 19 are in good agreement with data presented in reference 3 for
similar semispan models at the same Reynolds numbers and Mach numbers.
Since analysis of these data has already been made in reference 3, no
further discussion is included herein.

As was emphasized in reference 3, the aerodynamic characteristics
of both the plane wing and the cambered and twisted wing showed large
effects of Reynolds numbers at low speeds. It was therefore deemed
desirable to establish the extent to which the data were affected by
Reynolds number at high subsonic Mach numbers. To accomplish this end,
tests of the two full-span models were conducted in the Ames 12-foot

pressure tunnel at Reynolds numbers of 1,000,000 and 2,000,000 at Mach numbers up to 0.92, and similar tests of the same models were conducted in the Ames 16-foot high-speed wind tunnel at Reynolds numbers up to about 5,000,000. (See fig. 3.) The results of these tests are presented in figures 20 and 21.

Plane wing.- The data presented in figure 20 show that there were no large effects of Reynolds number on the aerodynamic characteristics of the plane wing for the range of Reynolds numbers and Mach numbers covered by this phase of the investigation. Lift and drag data obtained in the 12-foot pressure tunnel and the 16-foot wind tunnel at the same Reynolds number and Mach number do not show as good agreement as would be expected. Some of these differences may be attributed to differences in air-stream turbulence between the two facilities. A second factor which may contribute to this lack of agreement is the inexactness of the corrections for tunnel-wall interference.

Cambered and twisted wing.- The lift, drag, and pitching-moment characteristics of the model with the cambered and twisted wing (fig. 21) show that, for a Reynolds number of 2,000,000 and a Mach number of 0.25, the results obtained in the two wind tunnels agree well up to lift coefficients where large amounts of separation were present.

A substantial decrease in drag with increasing Reynolds number is noted at moderate and high angles of attack. At a Mach number of 0.80, increasing the Reynolds number from 1,000,000 to 4,700,000 decreased the lift coefficient at which the static instability first occurred, but at higher Mach numbers a slightly greater increase in Reynolds number resulted in a substantial increase in the value of this lift coefficient. Analysis of the data shows that, as the Reynolds number increased above 2,000,000 for a range of low positive lift coefficients, a forward movement of the center of pressure occurred; whereas at higher positive lift coefficients, above about 0.5, there was a rearward movement of the center of pressure. The large difference in pitching-moment characteristics indicates that the type and extent of the boundary-layer separation on the wing was strongly affected by Reynolds number.

Effects of Surface Roughness

The effects of surface roughness on the aerodynamic characteristics of the two wings are presented in figures 22 and 23. Surface roughness consisted of a 1/8-inch strip of number 60 carborundum at the 10-percent chord line on both upper and lower surfaces of the wing. The data were obtained in the Ames 16-foot wind tunnel.

Addition of surface roughness had little effect on the aerodynamic characteristics of the plane wing. Tests in the 12-foot tunnel of a similar wing with surface roughness (reference 3) likewise showed little effect of roughness on the aerodynamic characteristics.

The addition of the same type of roughness to the cambered and twisted wing had only a small effect on the lift and drag at low Mach numbers, but as the Mach number and Reynolds number increased, the effects of roughness became large. At Mach numbers of 0.80 and above, the addition of roughness resulted in a more linear variation of lift coefficient with angle of attack and a higher drag at moderate lift coefficients. Adding roughness to the model produced large changes in the pitching-moment characteristics, especially at the higher Mach numbers. The model with roughness did not show the extreme Mach number effects that characterized the smooth model on which, at the higher Mach numbers, the center of pressure moved rearward as the lift coefficient increased prior to the occurrence of static instability. At Mach numbers of 0.80 and above, the addition of surface roughness resulted in a decrease in the lift coefficient at which severe static longitudinal instability occurred.

CONCLUDING REMARKS

The lift and drag measured on the full-span and the semispan models having the same wing configuration were in good agreement. In general, the aerodynamic center of the semispan models was slightly rearward of its position on the full-span model.

Increasing the Reynolds number over the Mach number range had only a small effect on the characteristics of the plane wing. The data for the cambered and twisted wing indicate that increasing the Reynolds number at the higher Mach numbers resulted in an increase in the lift coefficient at which the static instability first occurred, and also caused a forward movement of the center of pressure at low positive lift coefficients and a rearward movement of center of pressure at higher lift coefficients.

Addition of surface roughness had little effect on the aerodynamic characteristics of the plane wing. At Mach numbers of 0.80 and above, the same type of roughness applied to the cambered and twisted wing resulted in a more linear variation of lift coefficient with angle of attack and reduced the lift coefficient at which the wing became unstable.

Ames Aeronautical Laboratory,
    National Advisory Committee for Aeronautics,
        Moffett Field, Calif.

REFERENCES

1. Hunton, Lynn W.: Effects of Twist and Camber on the Low-Speed
     Characteristics of a Large-Scale 45° Swept-Back Wing.
     NACA RM A50A10, 1950.

2. Hunton, Lynn W., and Dew, Joseph K.: The Effect of Camber and
     Twist on the Aerodynamic Loading and Stalling Characteristics
     of a Large-Scale 45° Swept-Back Wing. NACA RM A50J24, 1950.

3. Johnson, Ben H., Jr., and Shibata, Harry H.: Characteristics
     Throughout the Subsonic Speed Range of a Plane Wing and of a
     Cambered and Twisted Wing, Both Having 45° of Sweepback.
     NACA RM A51D27, 1951.

4. Cahill, Jones F.: Comparison of Semispan Data Obtained in the
     Langley Two-Dimensional Low-Turbulence Pressure Tunnel and Full-
     Span Data Obtained in the Langley 19-Foot Pressure Tunnel for a
     Wing With 40° Sweepback of the 0.27-Chord Line. NACA RM L9B25a,
     1949.

5. Lipson, Stanley, and Barnett, U. Reed, Jr.: Comparison of Semispan
     and Full-Span Tests of a 47.5° Sweptback Wing with Symmetrical
     Circular-Arc Sections and Having Drooped-Nose Flaps, Trailing-
     Edge Flaps, and Ailerons. NACA RM L51H15, 1951.

6. Loftin, Lawrence K., Jr.: Theoretical and Experimental Data for
     a Number of 6A-Series Airfoil Sections. NACA Rep. 903, 1948.
     (Formerly NACA RM L6J01 and NACA TN 1368.)

7. Olson, Robert N., and Mead, Merrill H.: Aerodynamic Study of a
     Wing-Fuselage Combination Employing a Wing Swept Back 63°. -
     Effectiveness of an Elevon as a Longitudinal Control and the
     Effects of Camber and Twist on the Maximum Lift-Drag Ratio at
     Supersonic Speeds. NACA RM A50A31a, 1950.

8. Silverstein, Abe, and White, James A.: Wind-Tunnel Interference
     With Particular Reference to Off-Center Positions of the Wing
     and to the Downwash at the Tail. NACA Rep. 547, 1935.

9. Sivells, James C., and Deters, Owen J.: Jet-Boundary and Plan-
     Form Corrections for Partial-Span Models with Reflection Plane,
     End Plate, or No End Plate in a Closed Circular Wind Tunnel.
     NACA Rep. 843, 1946. (Formerly NACA TN 1077.)

10. Herriot, John G.: Blockage Corrections for Three-Dimensional-Flow
     Closed-Throat Wind Tunnels, With Consideration of the Effect of
     Compressibility. NACA Rep. 995, 1950. (Formerly NACA RM A7B28.)

NACA 64A010 (plane wing)
NACA 64A810 (cambered
and twisted wing)

Pitching-moment axis
(0.25$\bar{c}$)

.818

$\frac{c'}{4}$

1.538

90°

$2r_o$=0.583

45°

r

x

b=6.484

1.453

1.802

1.542

$\bar{c}$=1.215

$\frac{l}{2}$=3.648

5.896

l=7.296

Twist distribution of the
cambered and twisted
wing

100

80

60

40

20

0

Spanwise station, percent
semispan
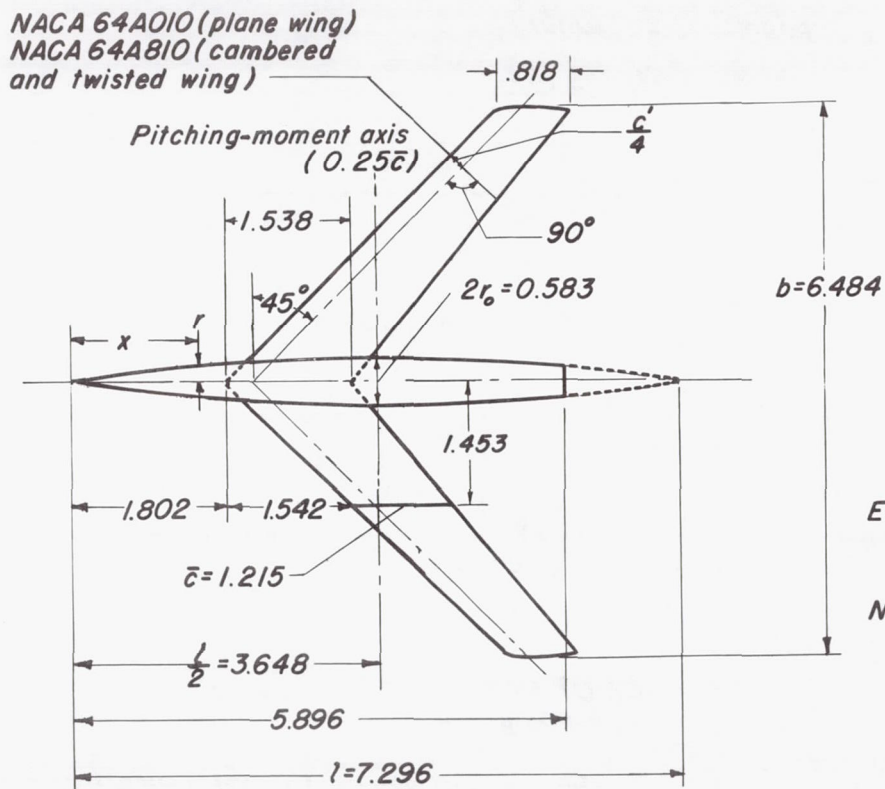
-10 -8 -6 -4 -2 0
Angle of twist, a_t, deg
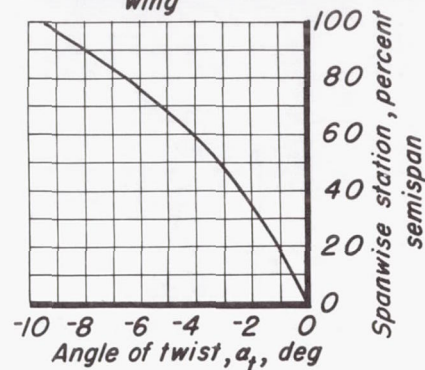
Equation for fuselage ordinates: $\dfrac{r}{r_o}=\left[1-\left(1-\dfrac{2x}{l}\right)^2\right]^{3/4}$

Note: All dimensions given in feet unless otherwise
specified.
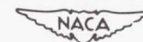
NACA

(a) Full-span models.

Figure 1.- Dimensional sketches of the models and the twist distribution of the cambered and twisted wing.

Aspect ratio 5.50
Taper ratio 0.53
Area semispan 3.81 ft^2

NACA 64A010 (plane wing)
NACA 64A810 (cambered and twisted wing)

0.818

Pitching-moment
axis (0.25$\bar{c}$)

$\frac{\bar{c}}{4}$

90°

$\bar{c}$ = 1.215

$\frac{b}{2}$ = 3.242

1.542

45°

1.453

r_0 = 0.292

r

x

1.802

1.538

$\frac{l}{2}$ = 3.648

5.896

l = 7.296

Equation for fuselage
ordinates:

$$\frac{r}{r_0} = \left[1 - \left(1 - \frac{2x}{l}\right)^2\right]^{3/4}$$

NACA
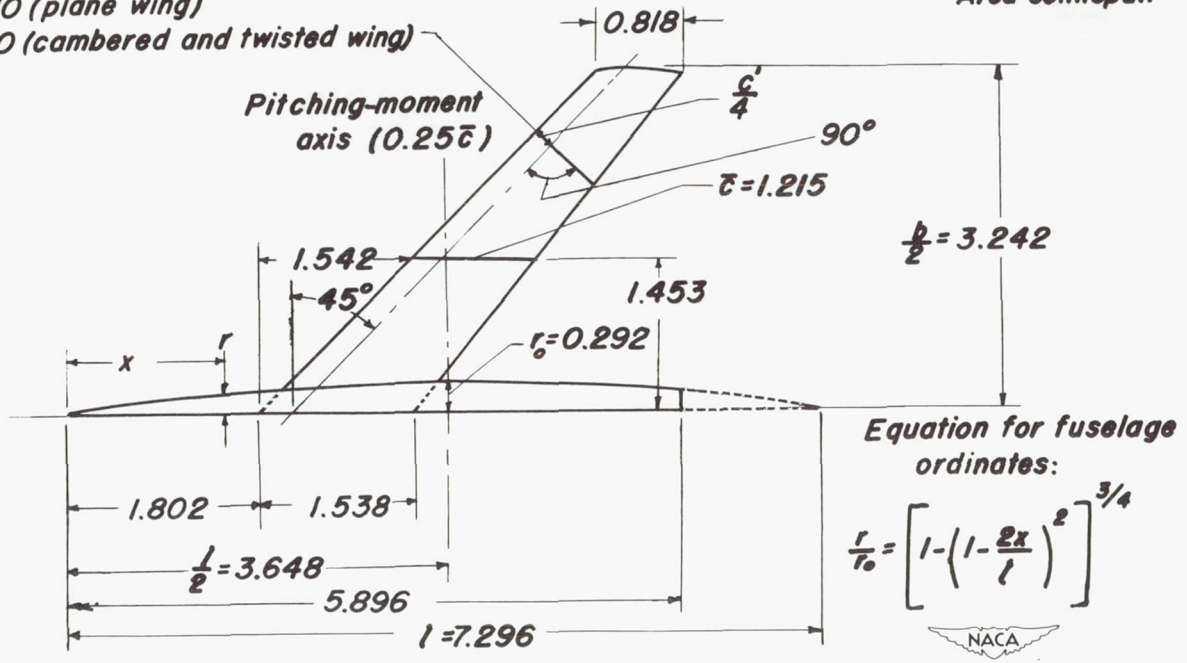
(b) Semispan models.

Figure 1.- Concluded.

(a) Full-span model.

Figure 2.— The model mounted in Ames 12-foot pressure wind tunnel.

(b) Semispan Model.

Figure 2.— Concluded.
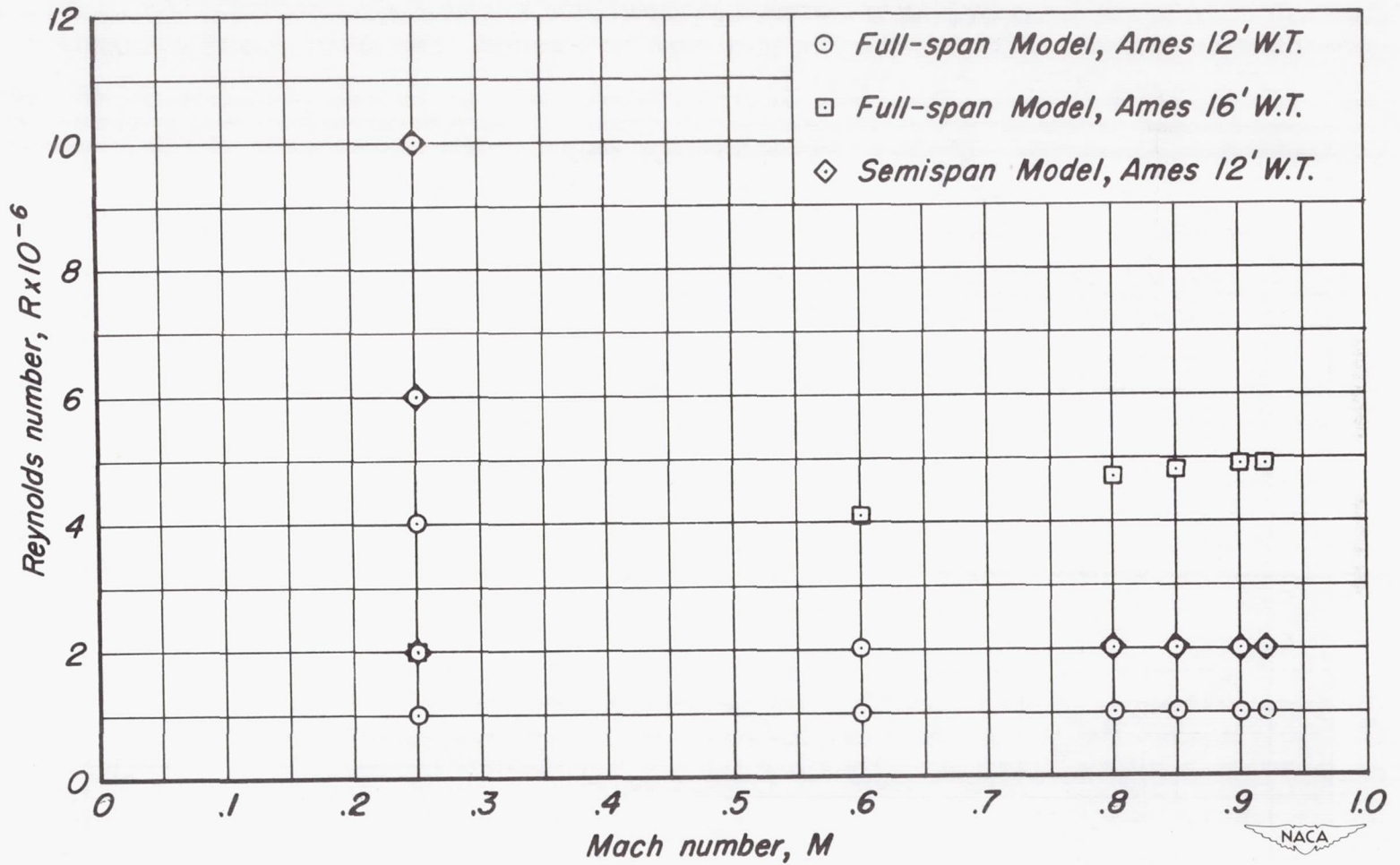
Figure 3.-The Mach numbers and Reynolds numbers of the tests.
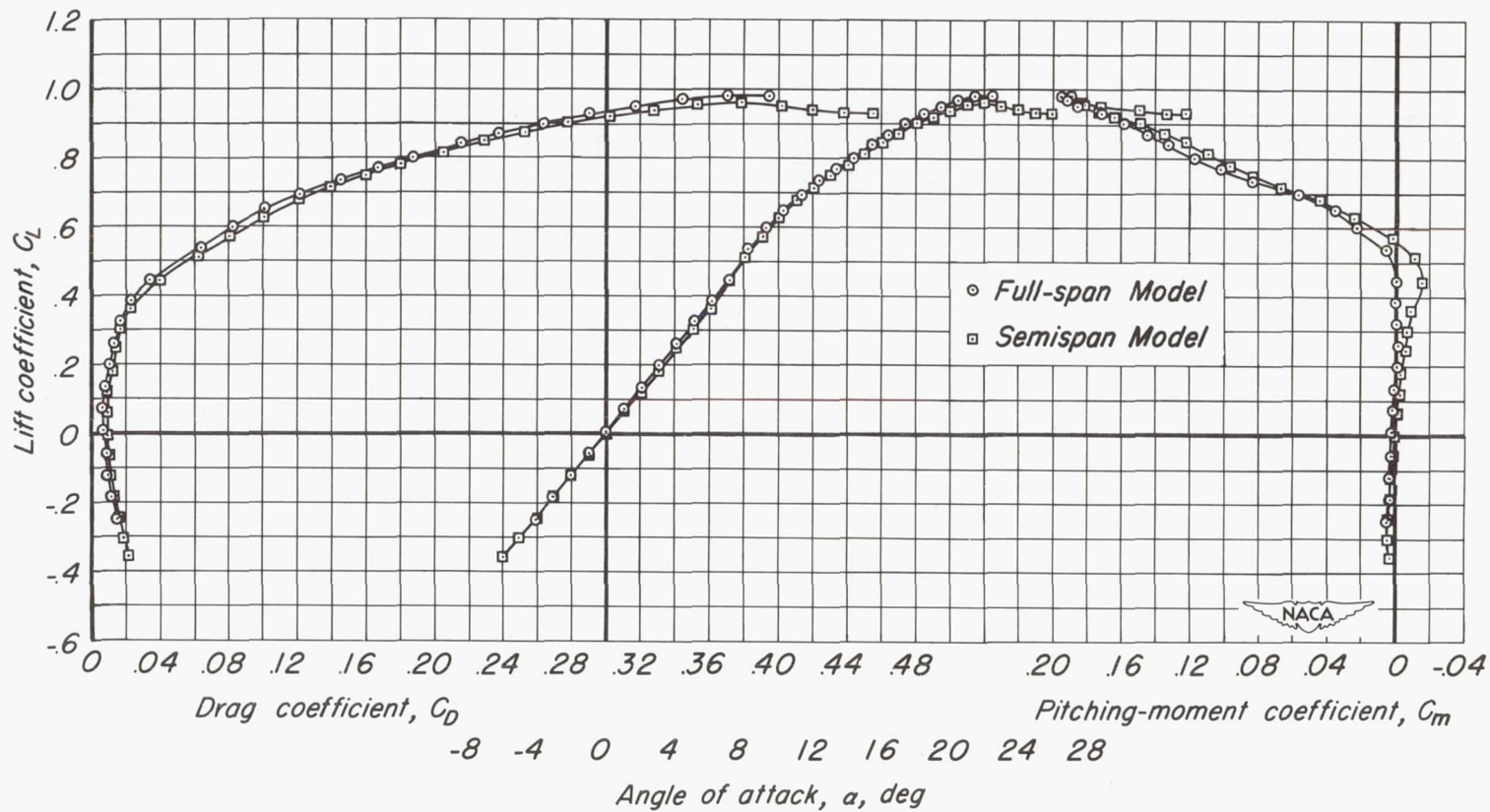
(a) M, 0.25

Figure 4.- Comparison of the aerodynamic characteristics of the full-span and semispan models having the plane wing at various Mach numbers. R, 2,000,000.
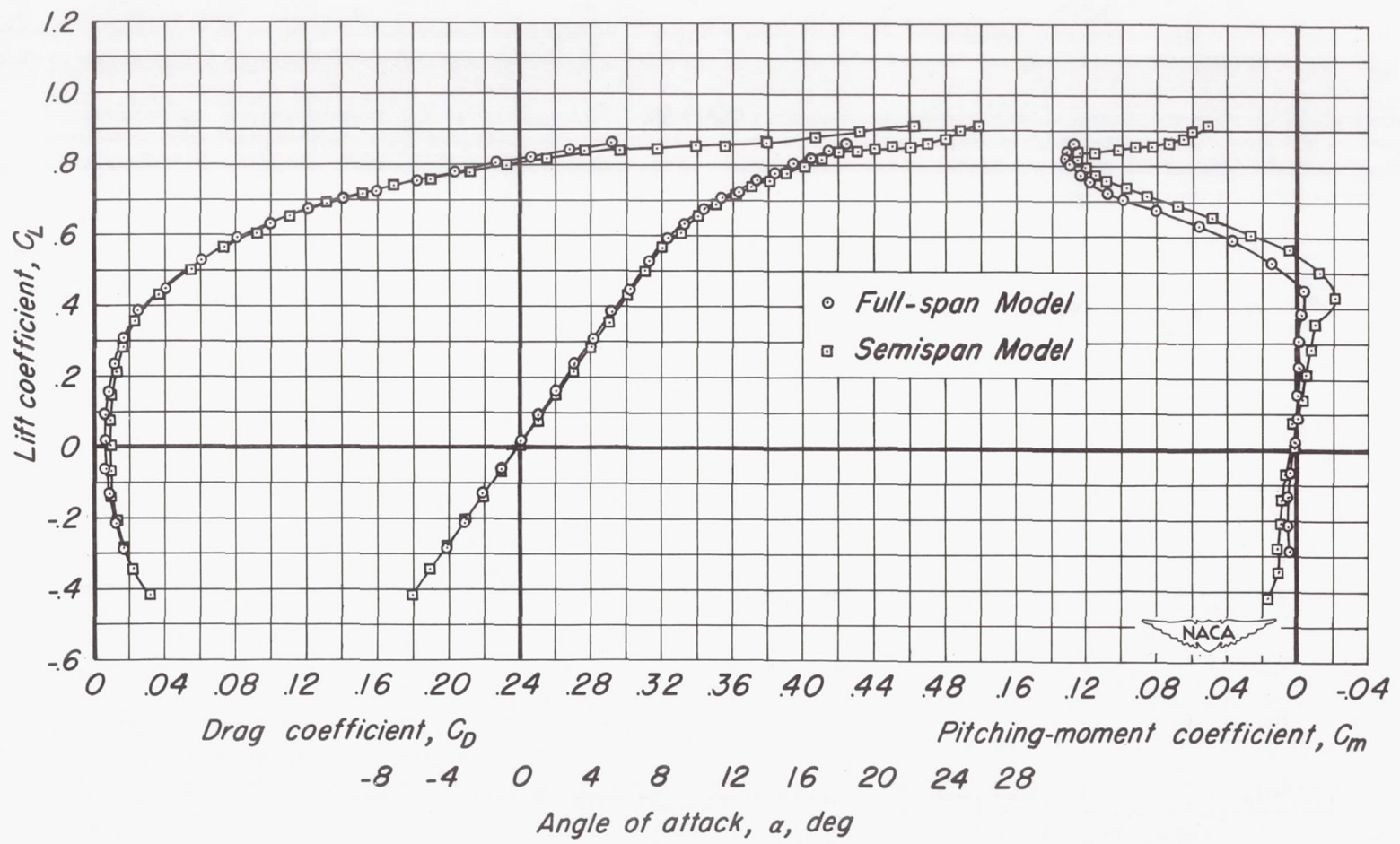
(b)   M, 0.80

Figure 4.- Continued.
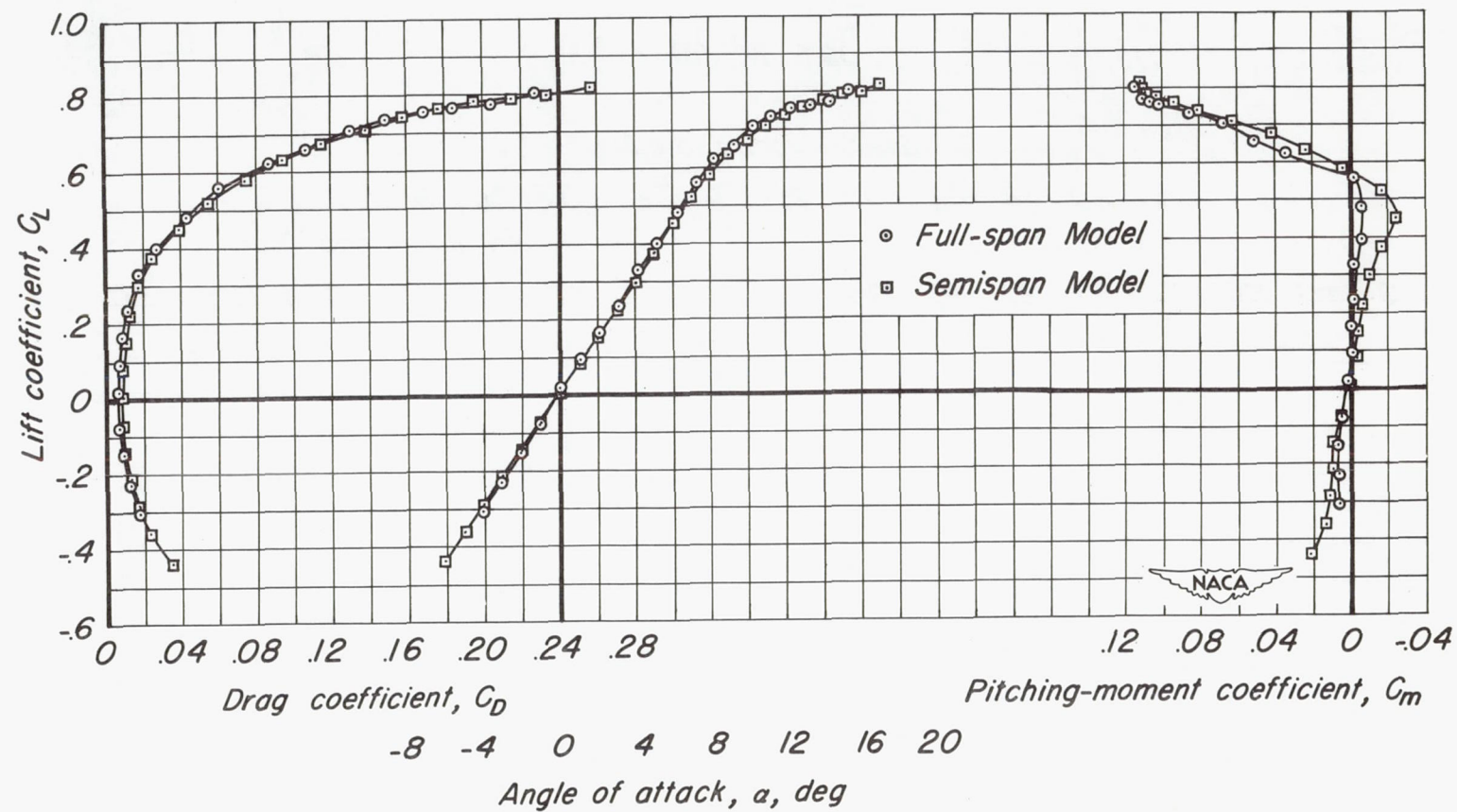
(c) M, 0.85

Figure 4.- Continued.
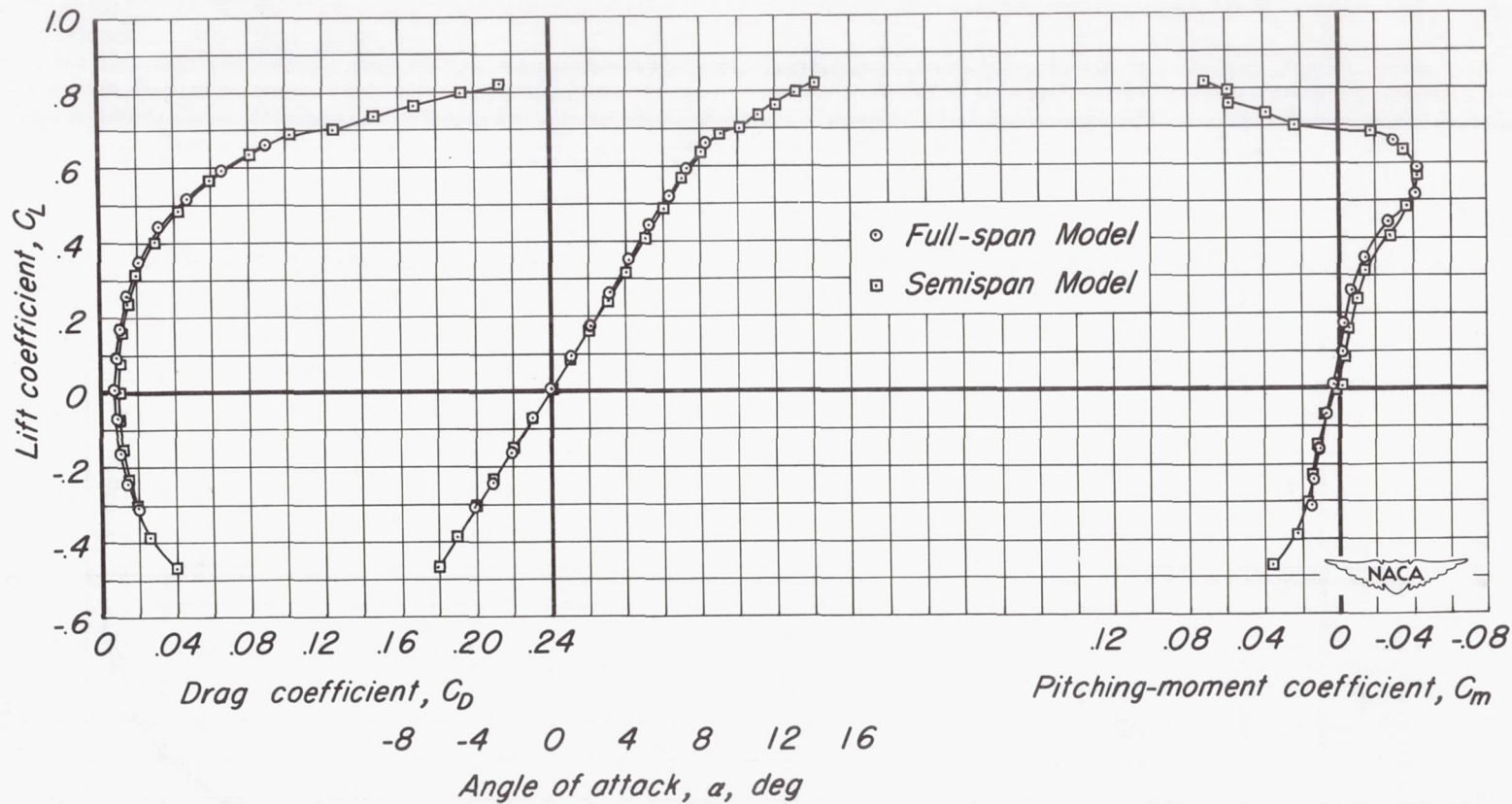
(d) M, 0.90

Figure 4.- Continued.
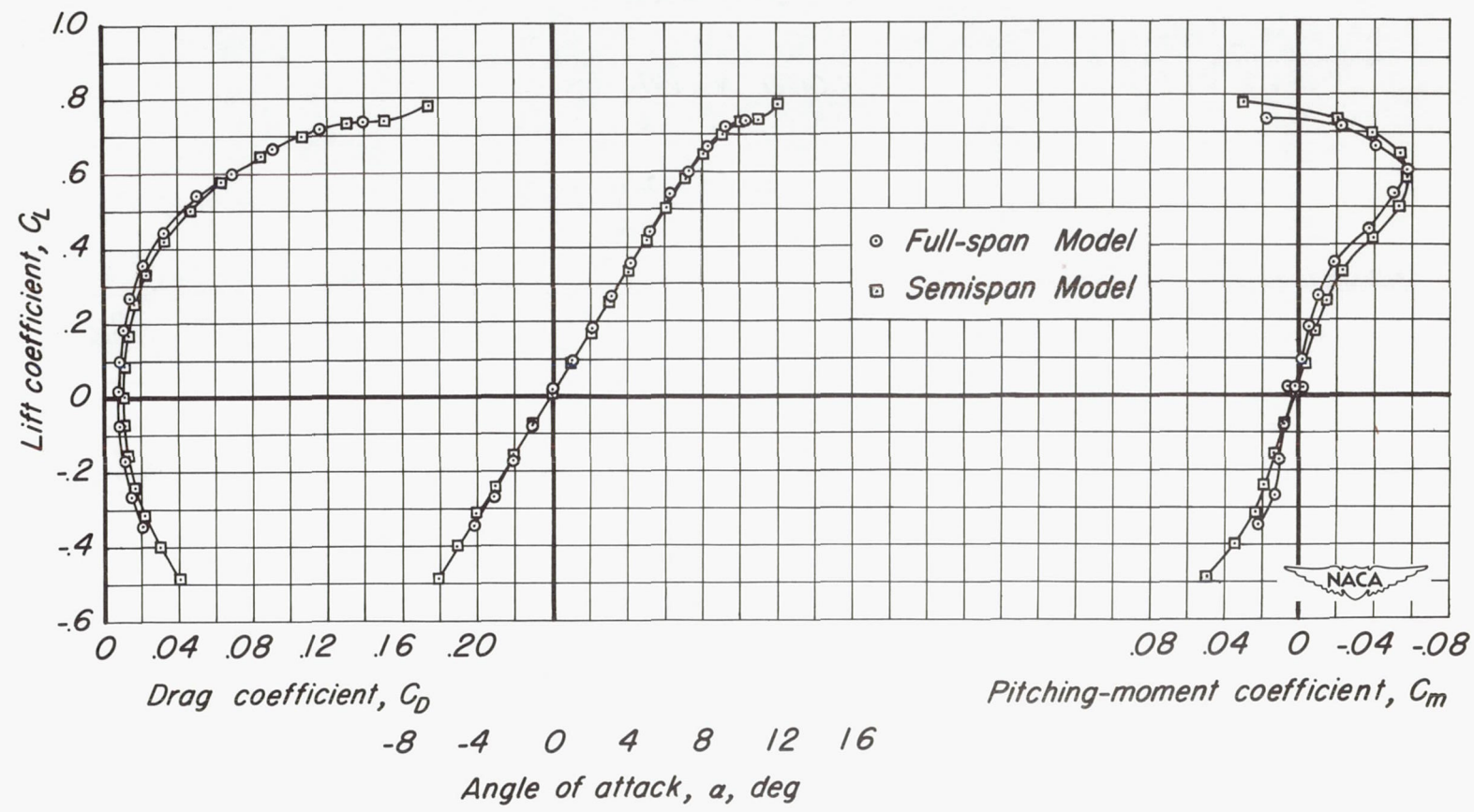
(e)   M, 0.92

Figure 4.- Concluded.
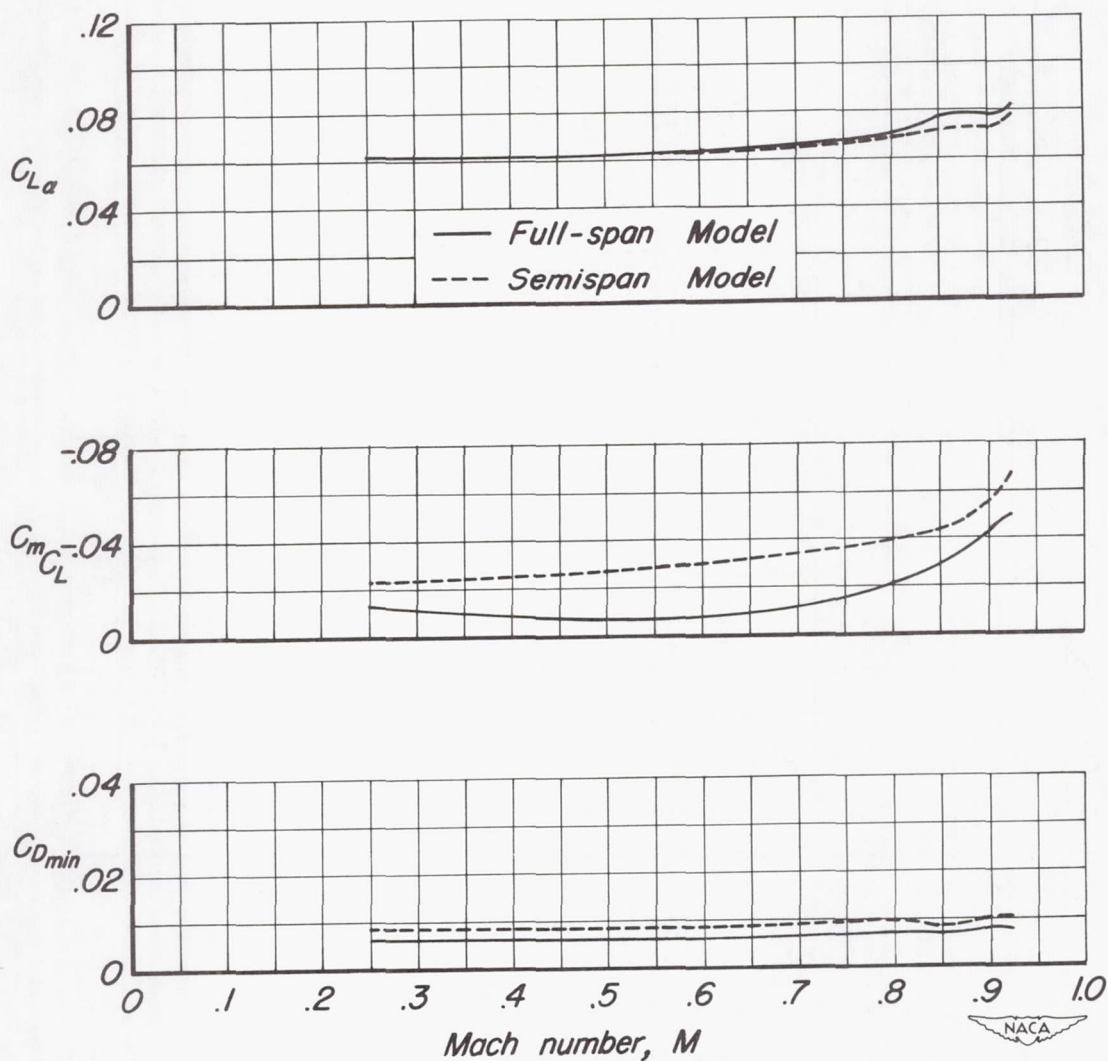
Figure 5.- The variation with Mach number of C_{L_α}, $C_{m_{C_L}}$, and $C_{D_{min}}$ for the full-span and semispan models with the plane wing. R, 2,000,000.
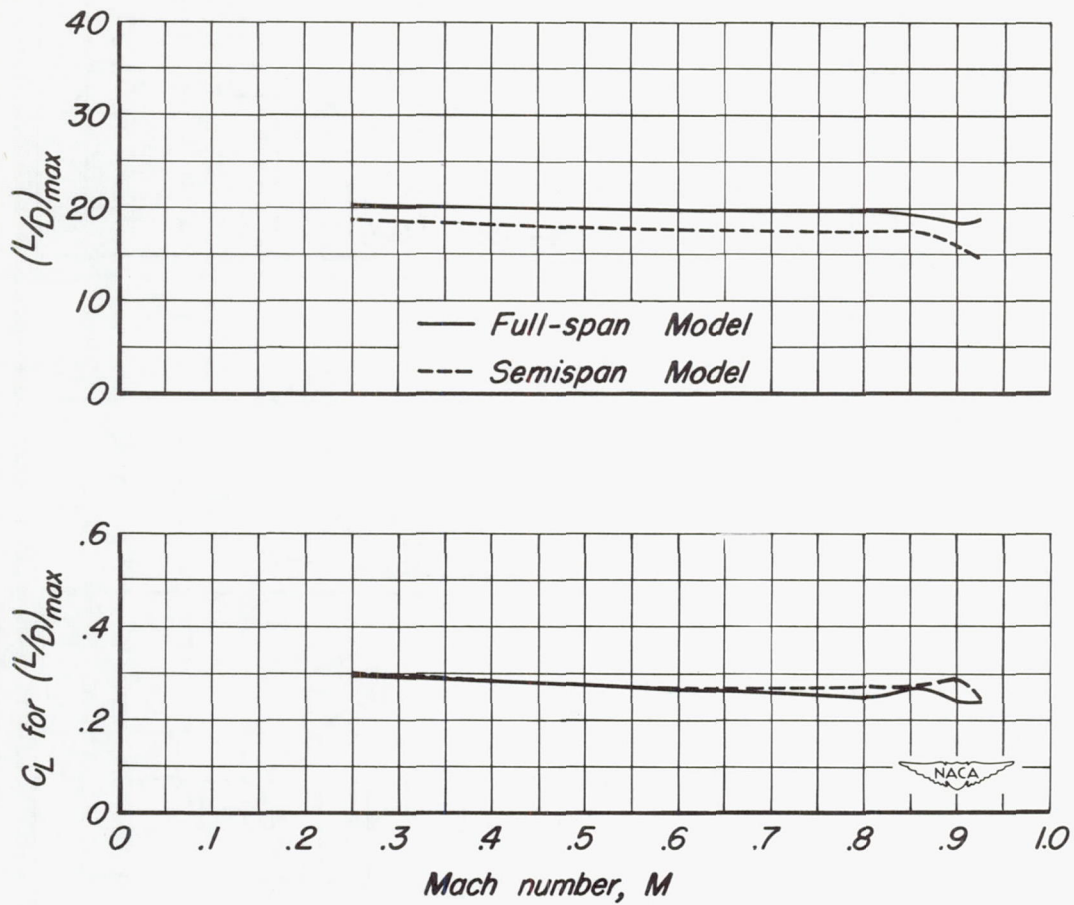
Figure 6.-The variation with Mach number of $(L/D)_{max}$ and C_L for $(L/D)_{max}$ for the full-span and semispan models with the plane wing. R, 2,000,000.

(a) R, 6,000,000
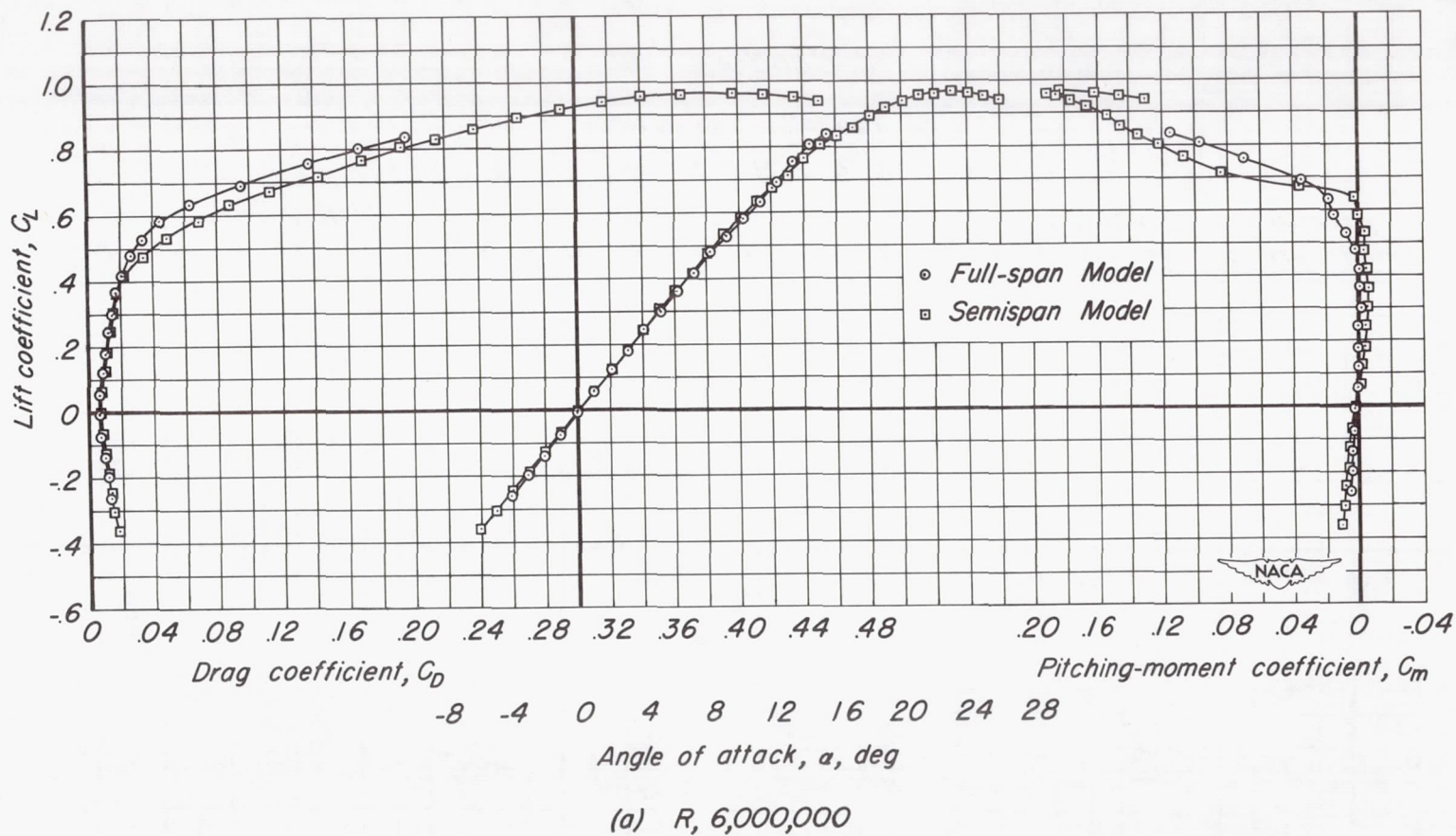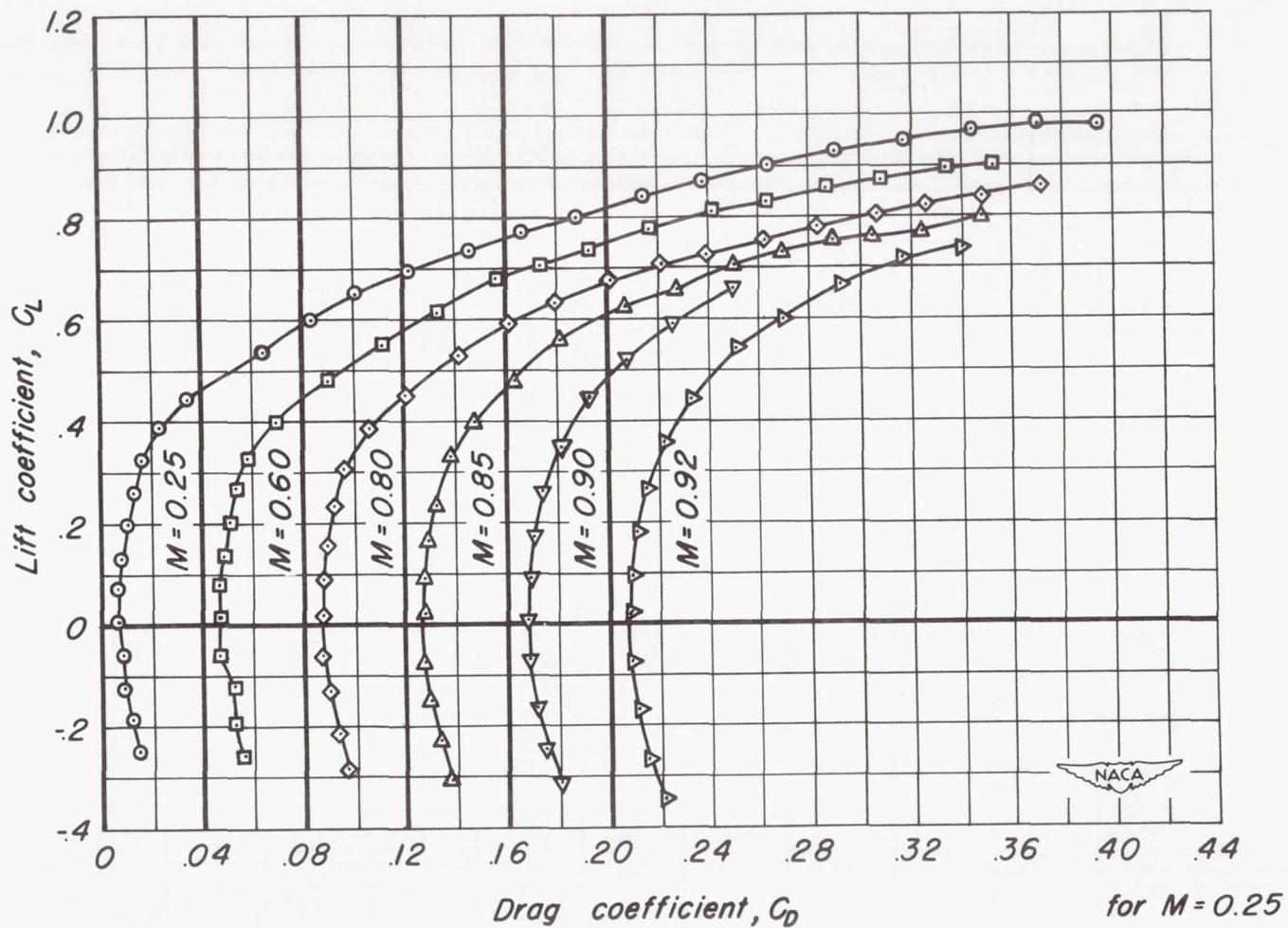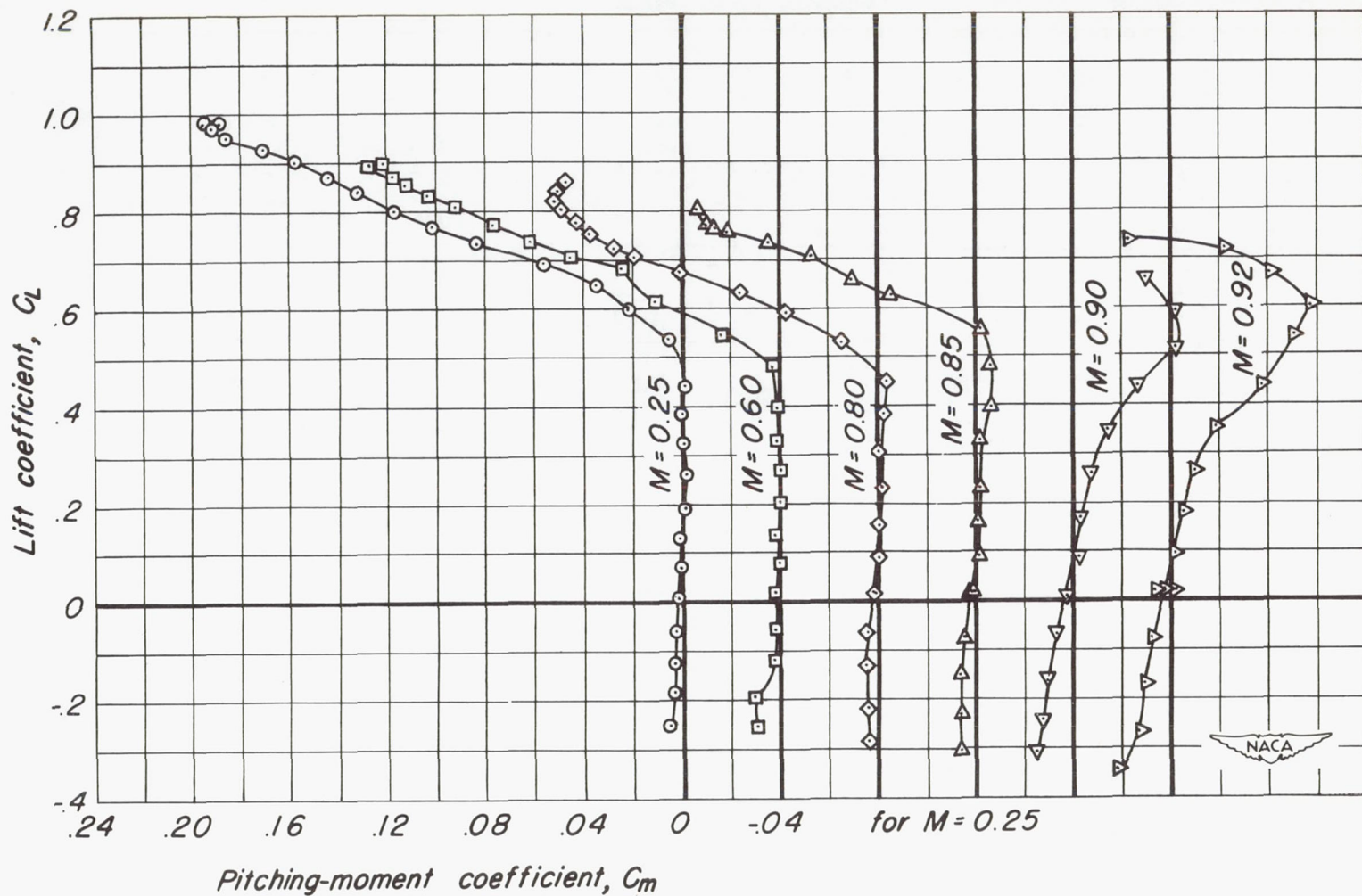
Figure 7.- Comparison of the aerodynamic characteristics of the full-span and semispan models having the plane wing at various Reynolds numbers. M, 0.25.
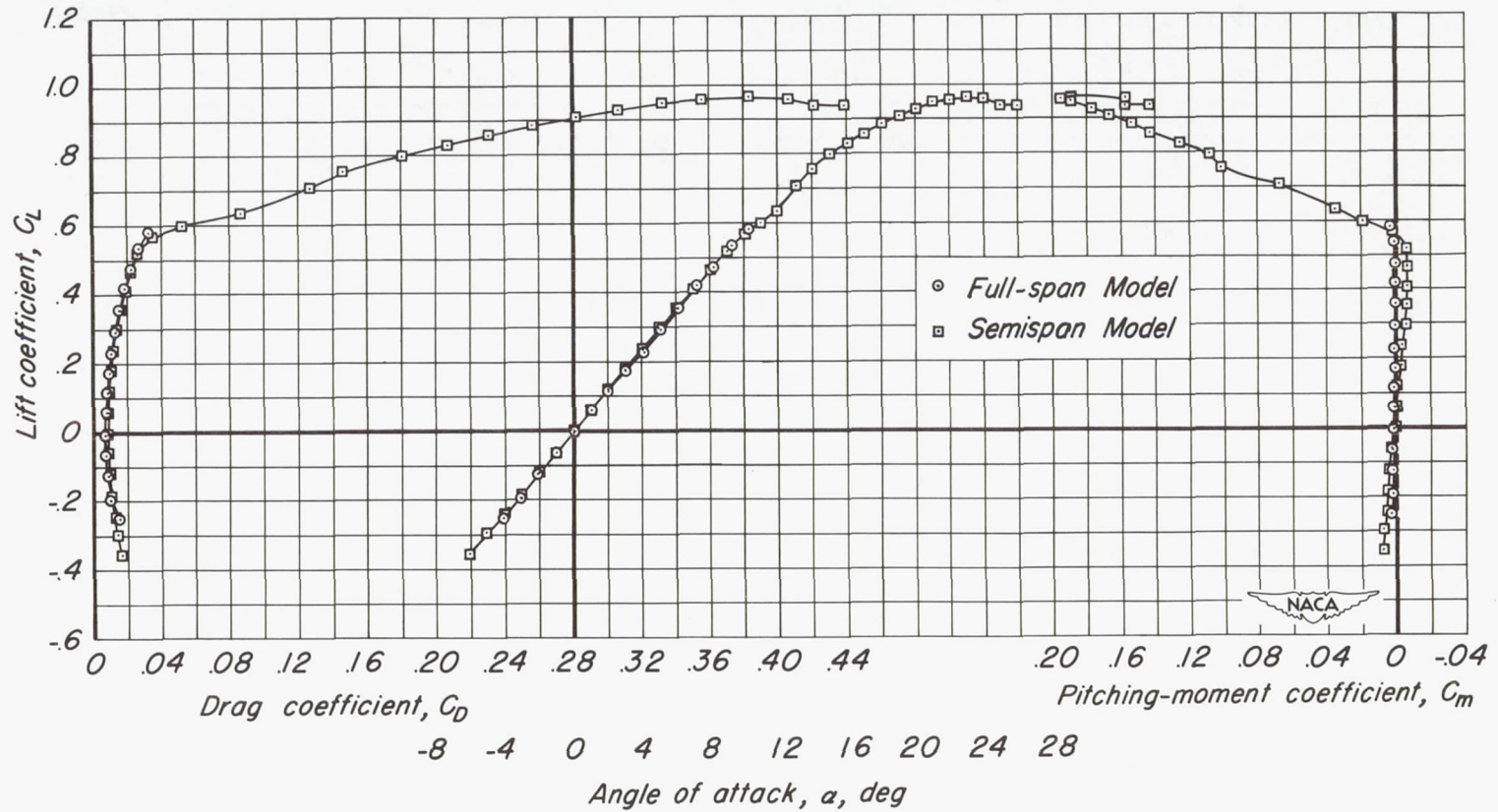
(b) R, 10,000,000.

Figure 7.- Concluded.
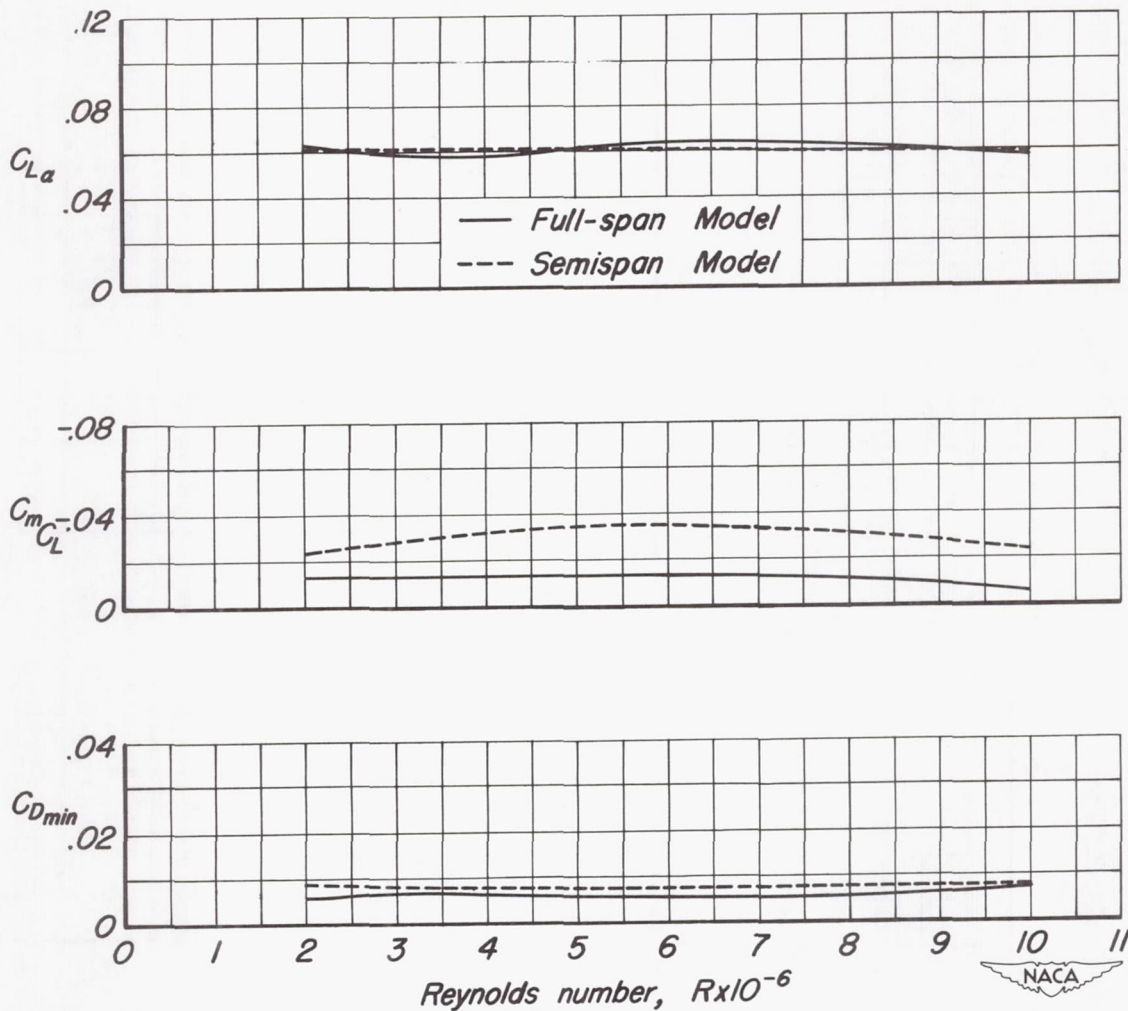
Figure 8.- The variation with Reynoids number of C_{L_α}, $C_{m_{C_L}}$, and $C_{D_{min}}$ for the full-span and semispan models with the plane wing.   M, 0.25.
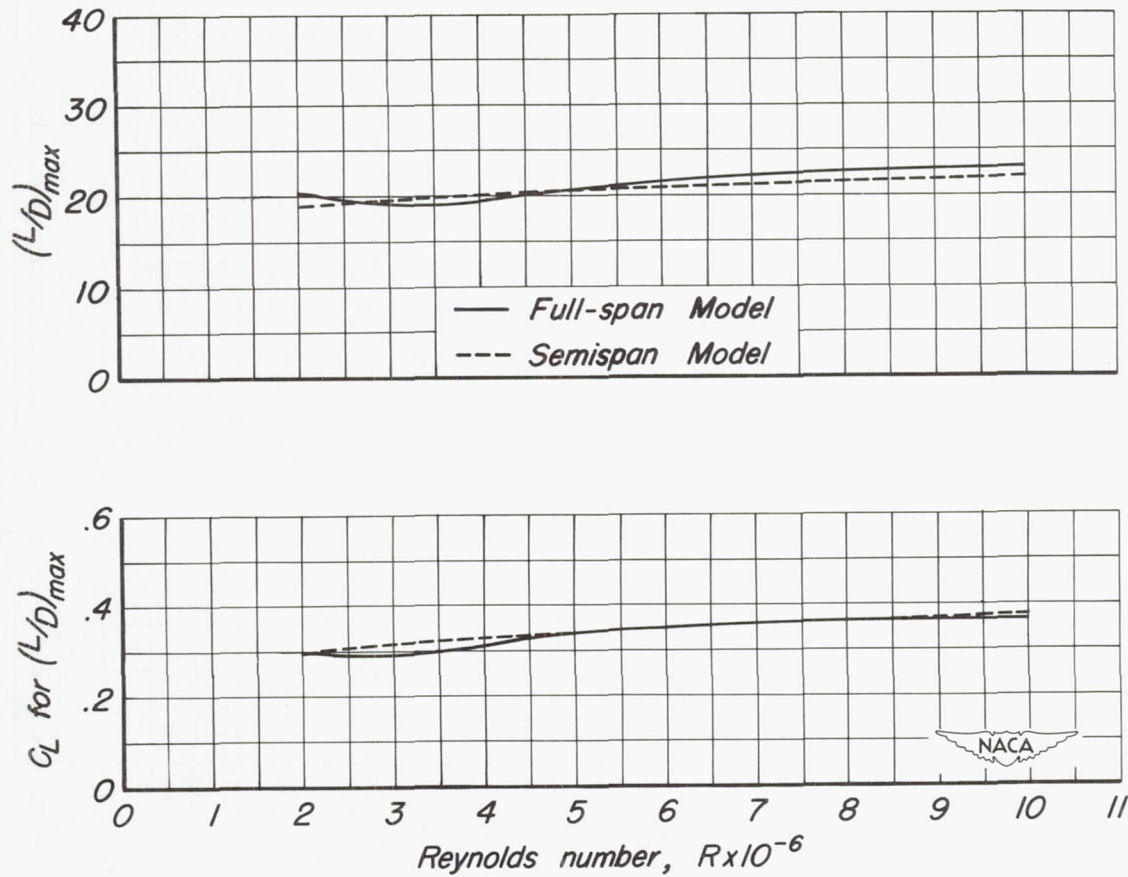
Figure 9.- The variation with Reynolds number of $(L/D)_{max}$ and C_L for $(L/D)_{max}$ for the full-span and semispan models with the plane wing. M, 0.25.
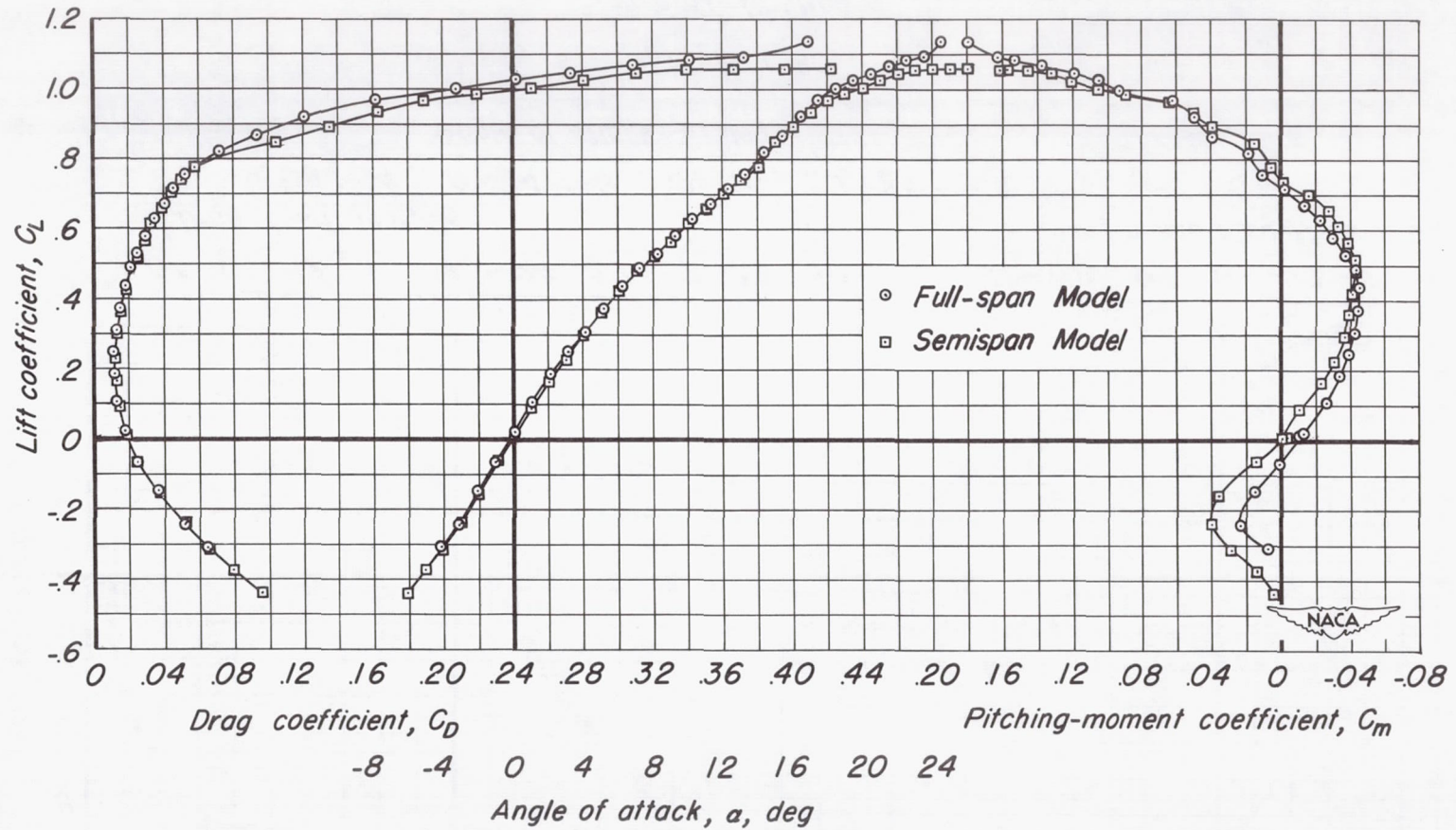
(a) M, 0.25

Figure 10.- Comparison of the aerodynamic characteristics of the full-span and semispan models having the
cambered and twisted wing at various Mach numbers. R, 2,000,000.
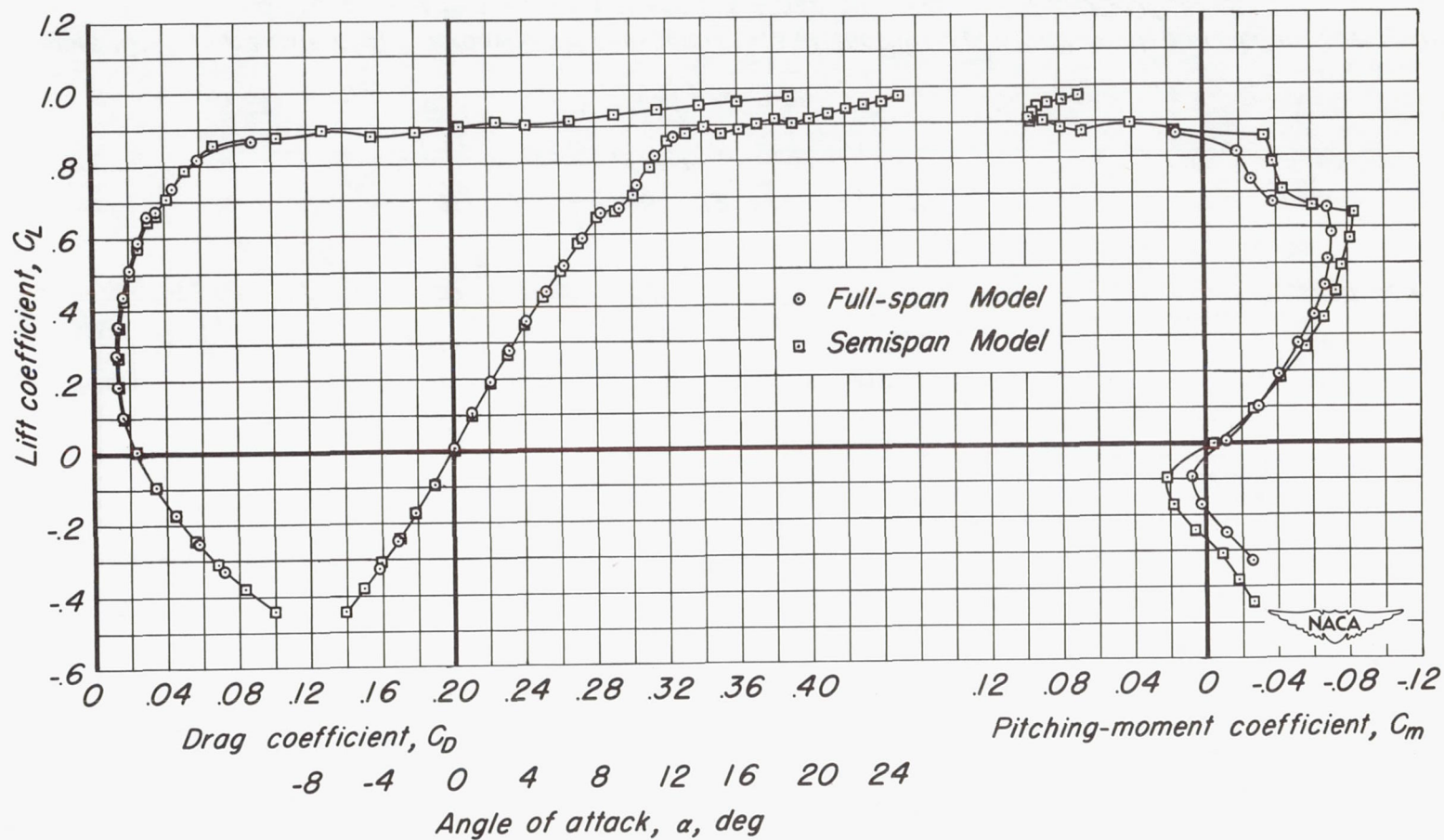
(b) M, 0.80

Figure 10.- Continued.
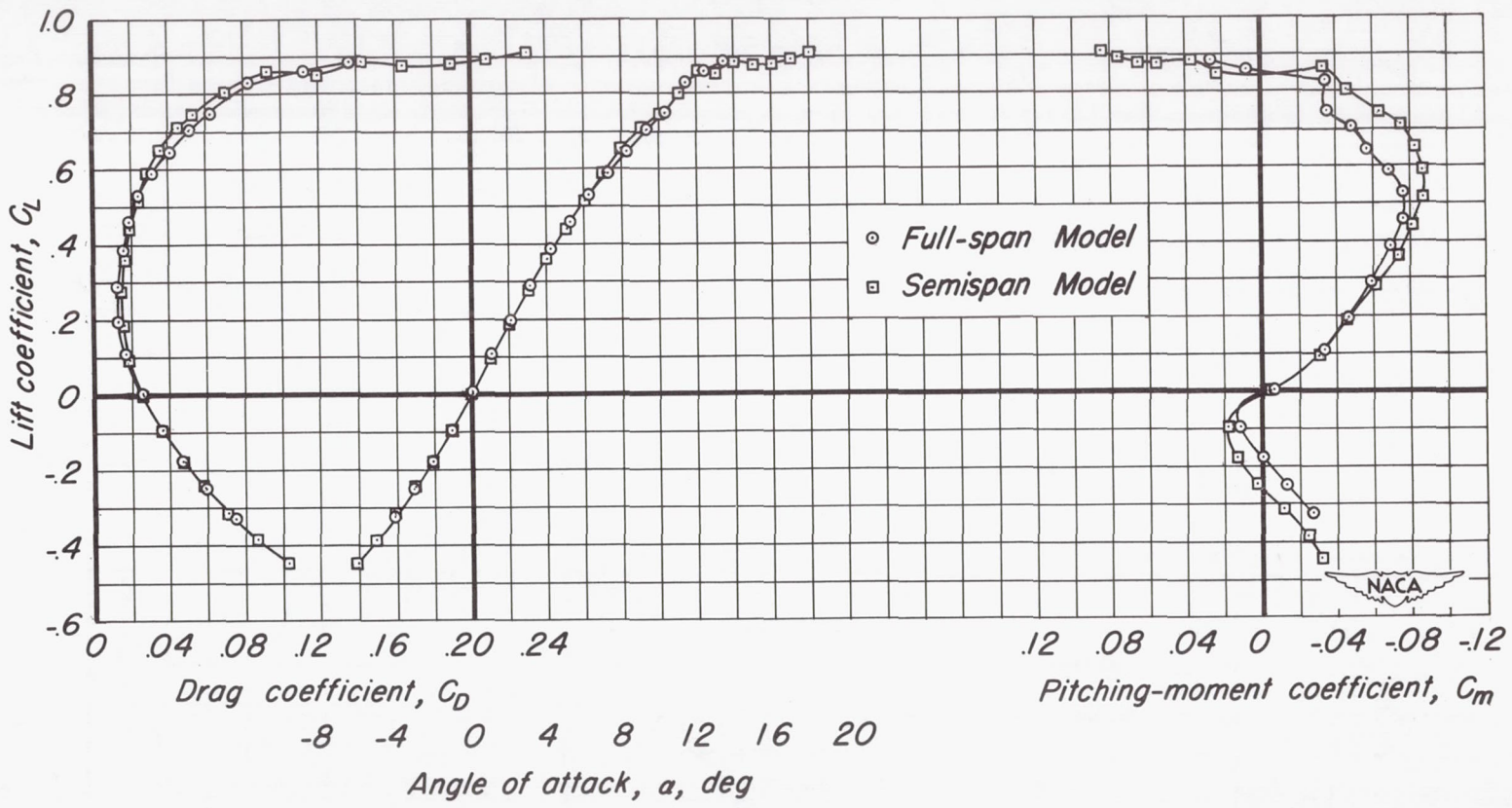
(c) M, 0.85

Figure 10.- Continued.
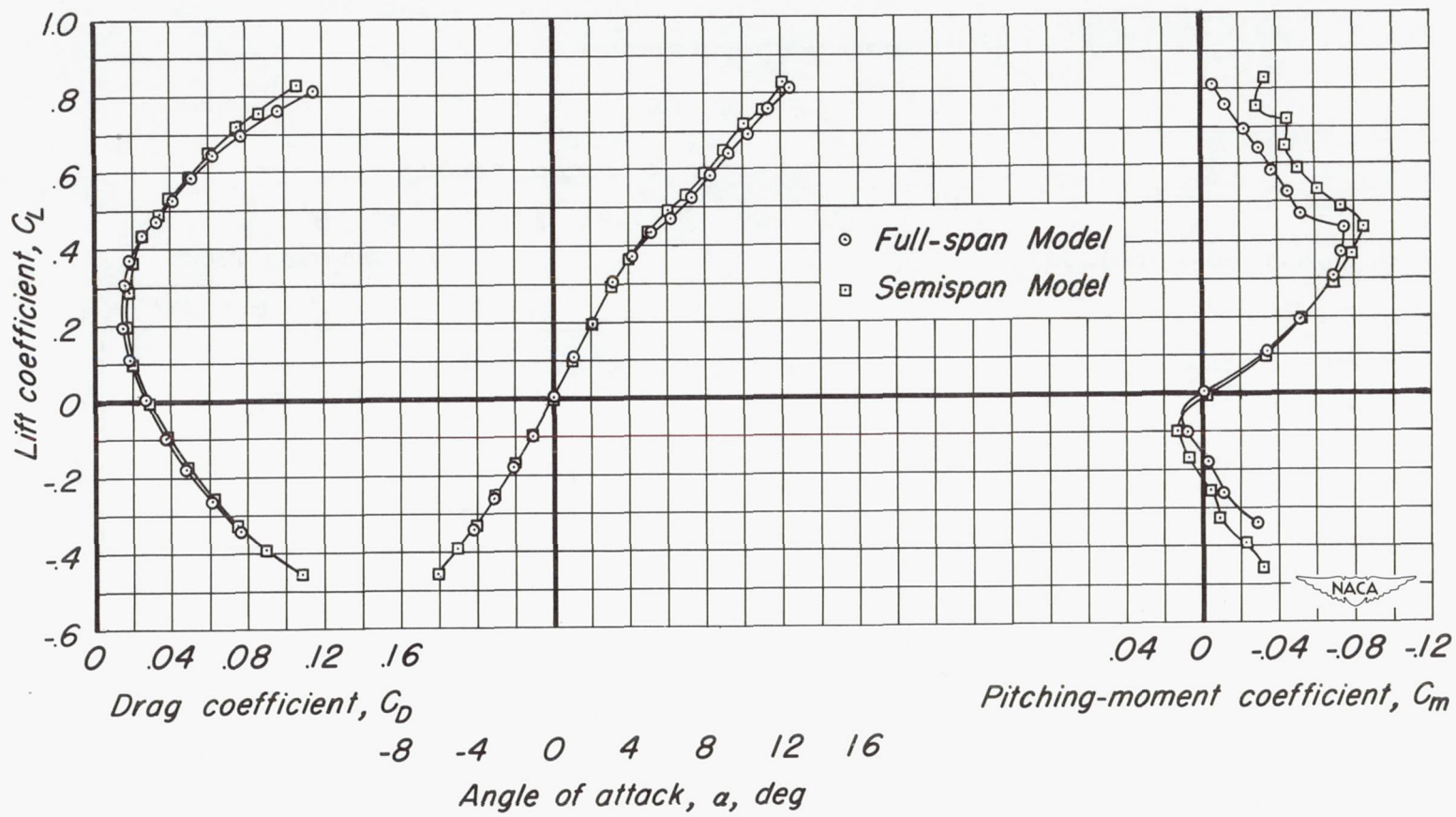
(d) M, 0.90

Figure 10.- Continued.
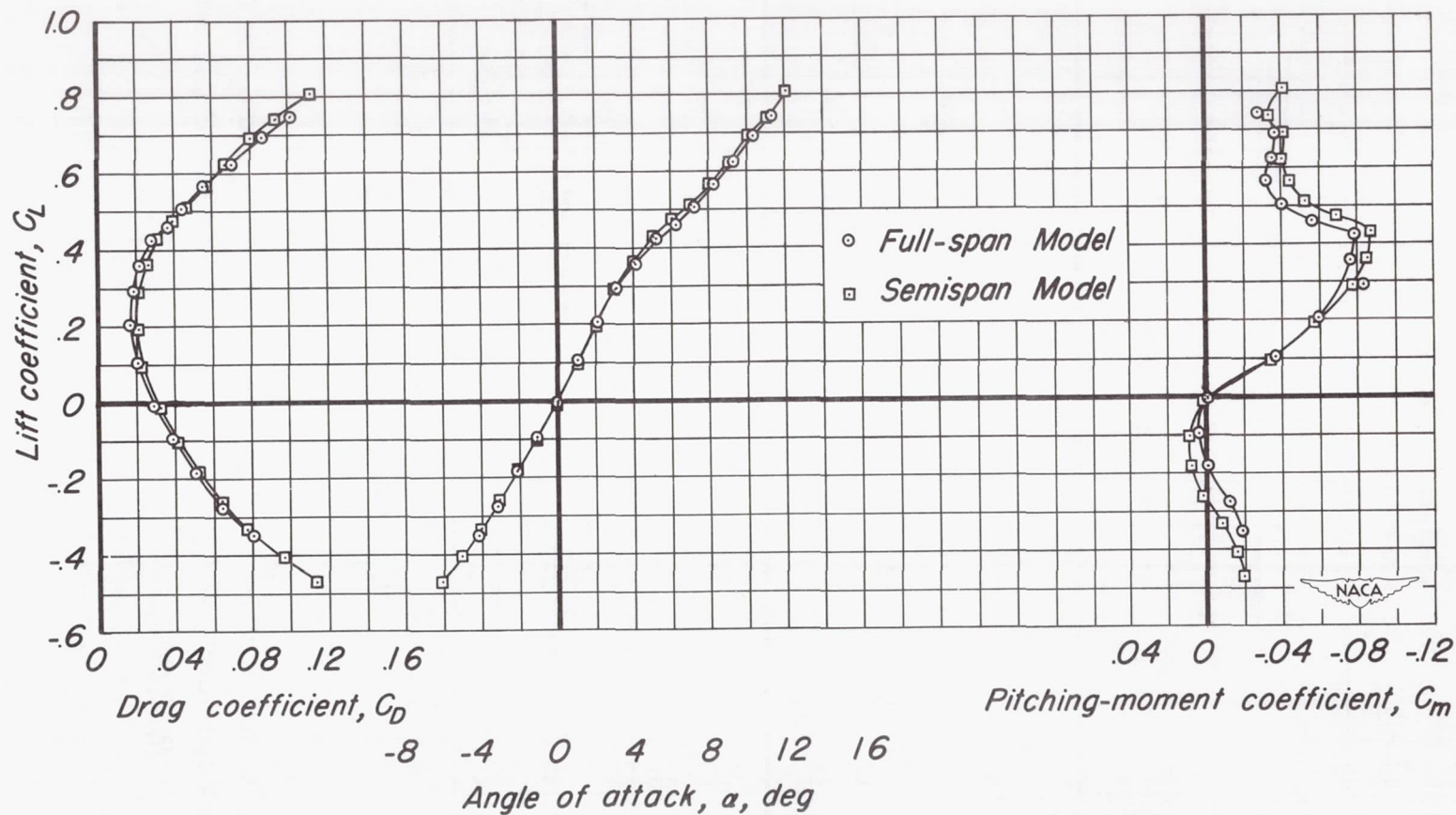
(e) M, 0.92

Figure 10.- Concluded.
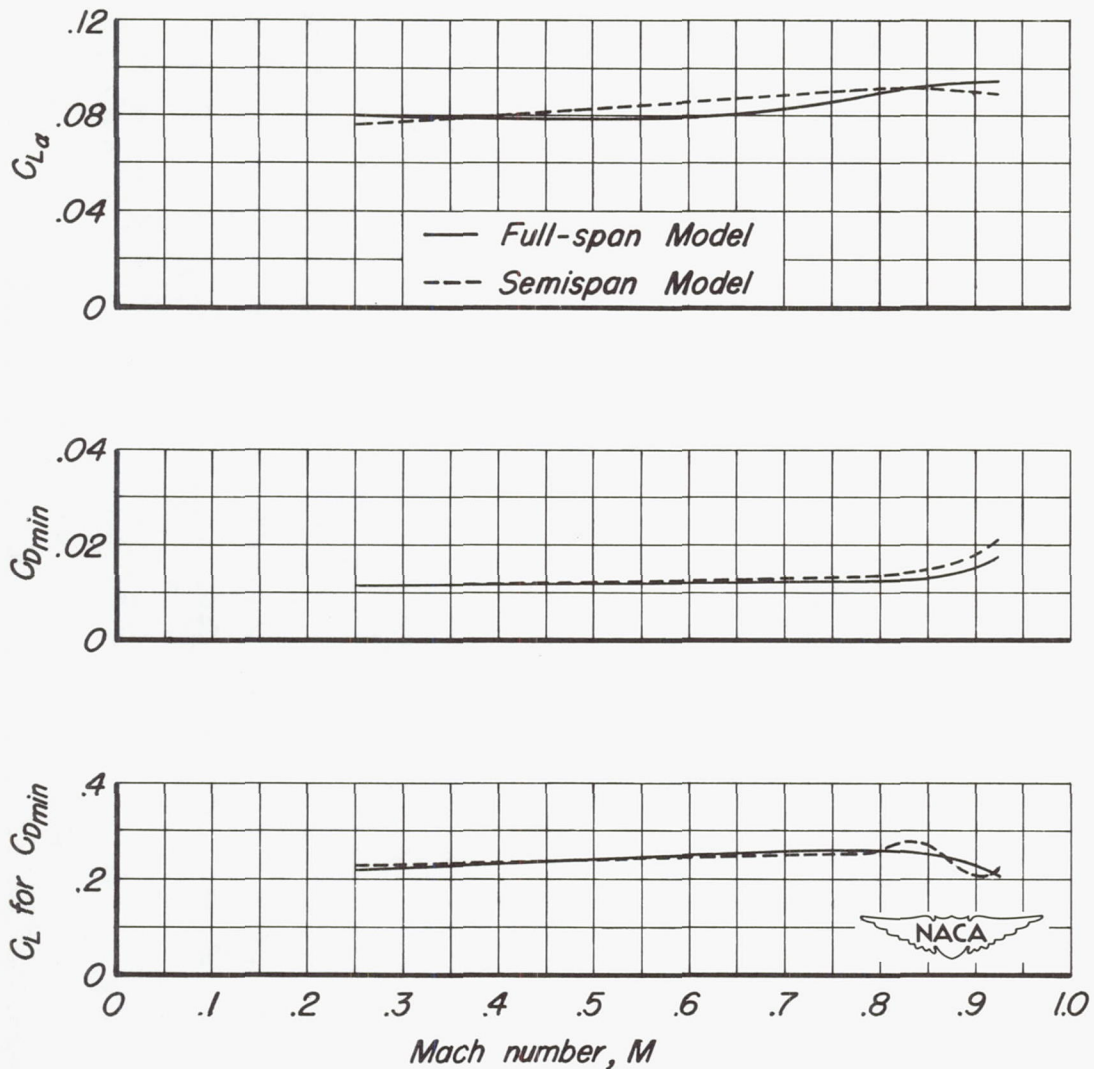
Figure 11.- The variation with Mach number of C_{L_α}, $C_{D_{min}}$, and C_L for $C_{D_{min}}$ for the full-span and semispan models with the cambered and twisted wing.   R, 2,000,000.
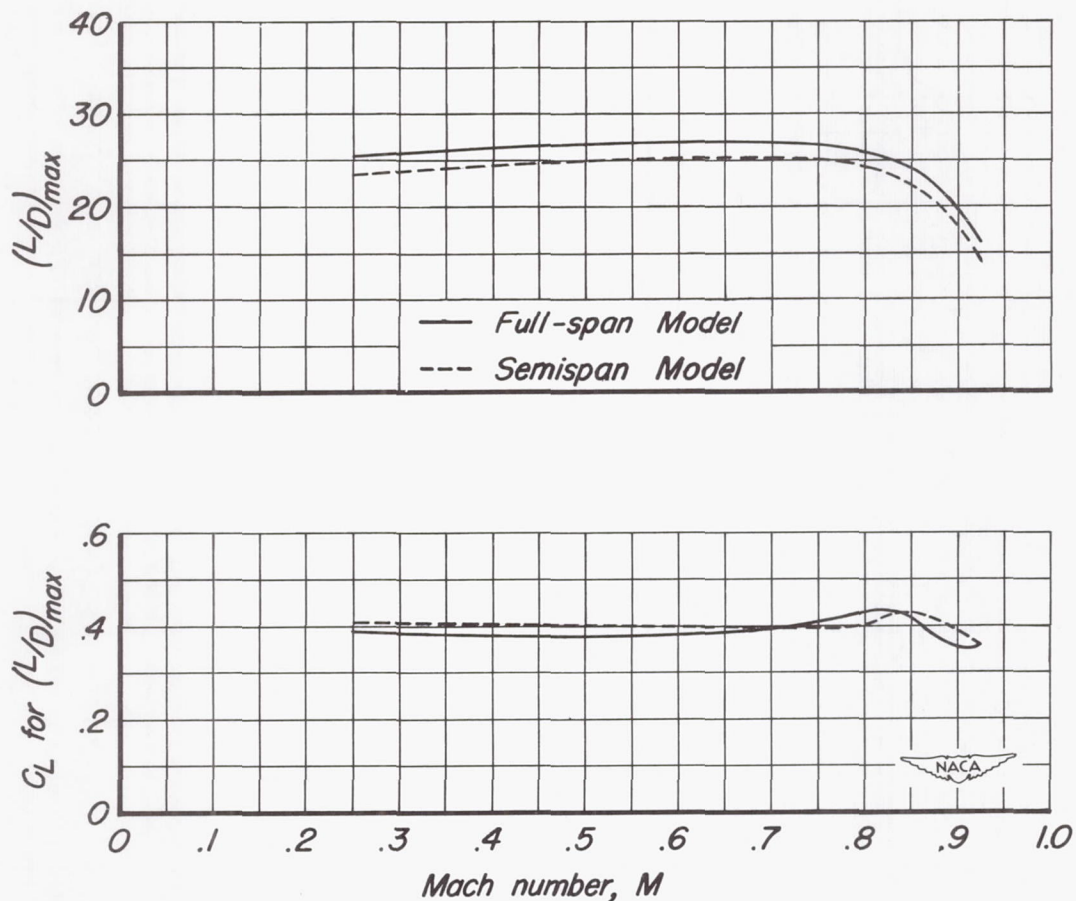
Figure 12.- The variation with Mach number of $(L/D)_{max}$ and C_L for $(L/D)_{max}$ for the full-span and semispan models with the cambered and twisted wing. R, 2,000,000.
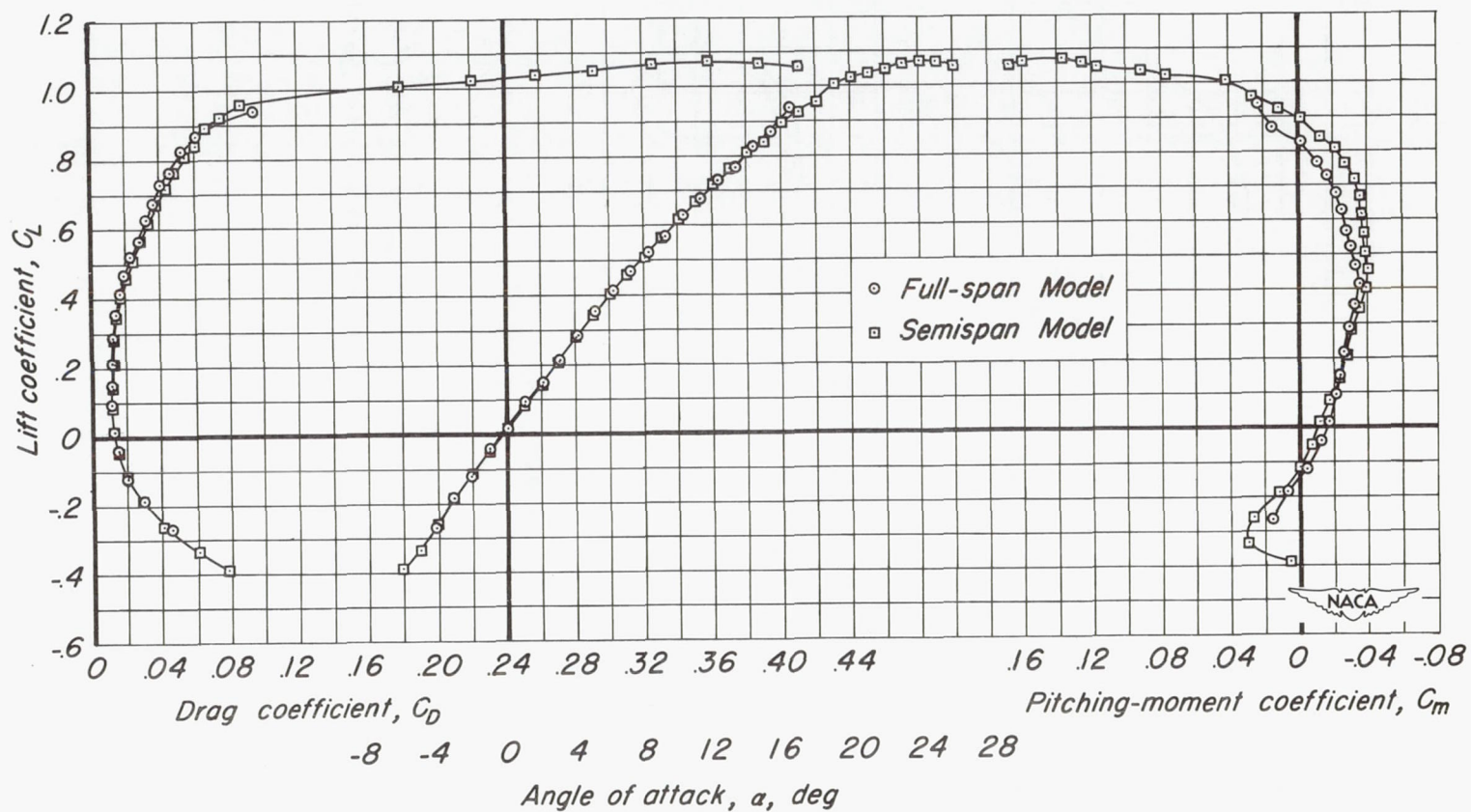
(a) R, 6,000,000

Figure 13.- Comparison of the aerodynamic characteristics of the full-span and semispan models having the cambered and twisted wing at various Reynolds numbers. M, 0.25.
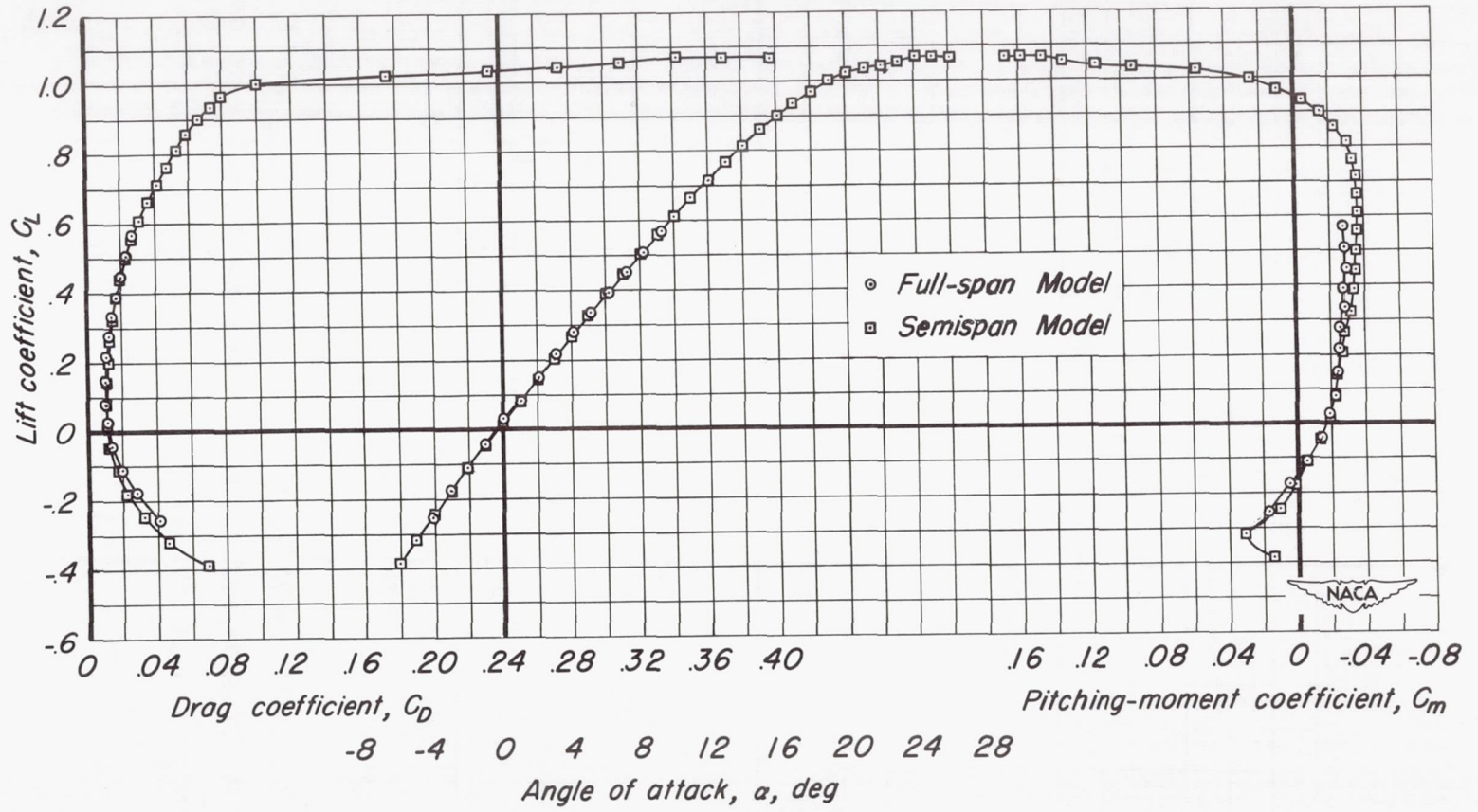
(b)   R, 10,000,000

Figure 13.- Concluded.
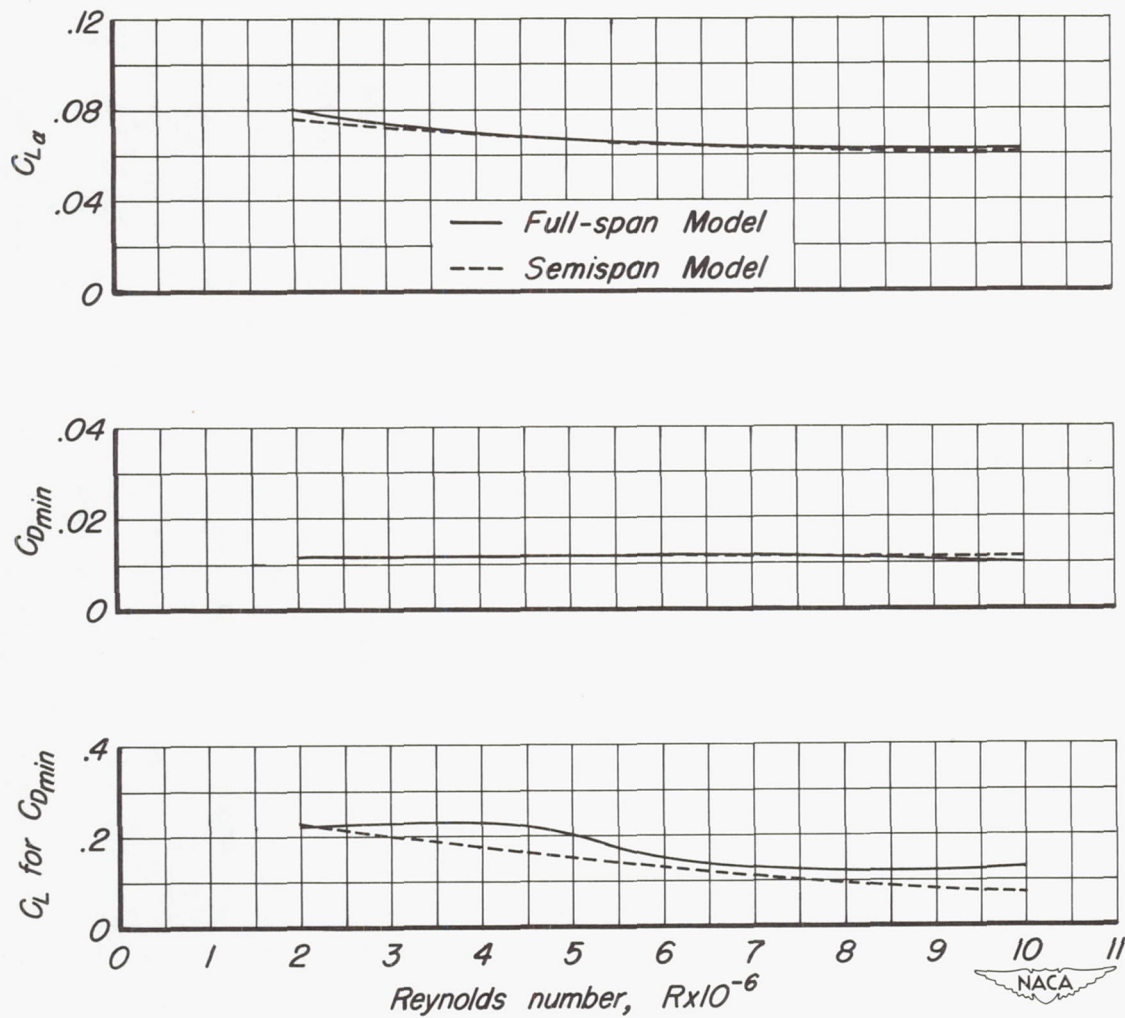
Figure 14.- The variation with Reynolds number of C_{L_a}, $C_{D_{min}}$, and C_L for $C_{D_{min}}$ for the full-span and semispan models with the cambered and twisted wing.   M, 0.25.
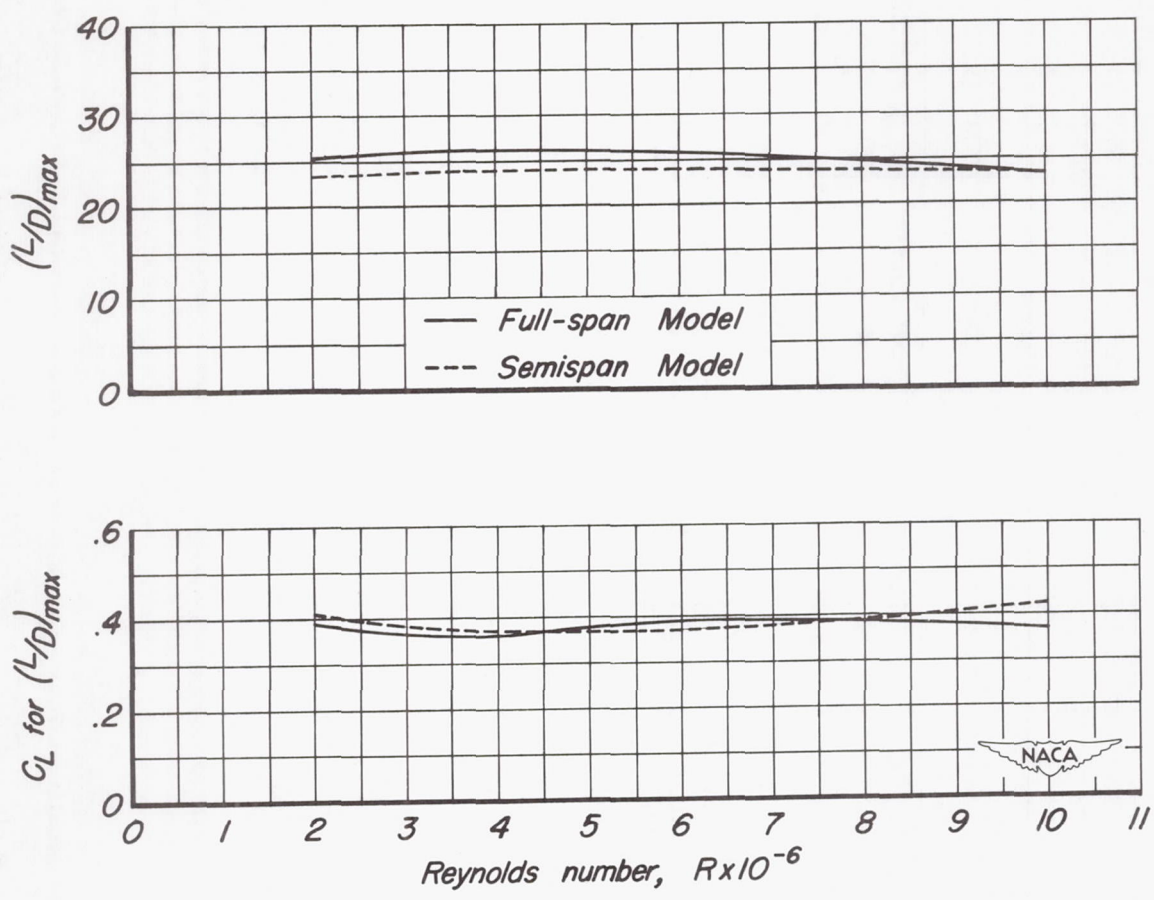
Figure 15.- The variation with Reynolds number of $(L/D)_{max}$ and C_L for $(L/D)_{max}$ for the full-span and semispan models with the cambered and twisted wing.   M, 0.25.
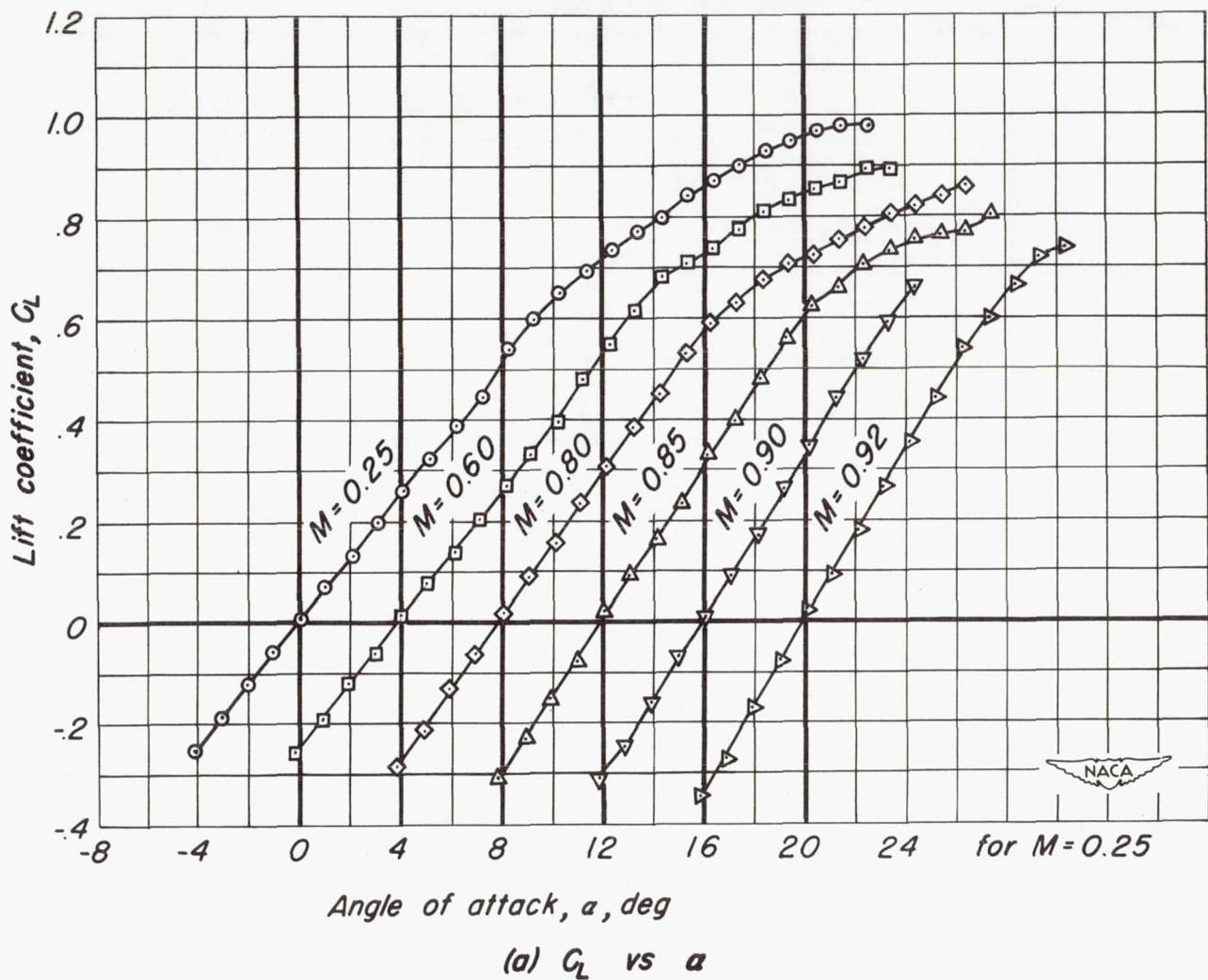
(a) C_L vs a

Figure 16.- The effect of Mach number on the aerodynamic characteristics of the full-span model with the plane wing at a Reynolds number of 2,000,000.

(b) C_L vs C_D

Figure 16.- Continued.
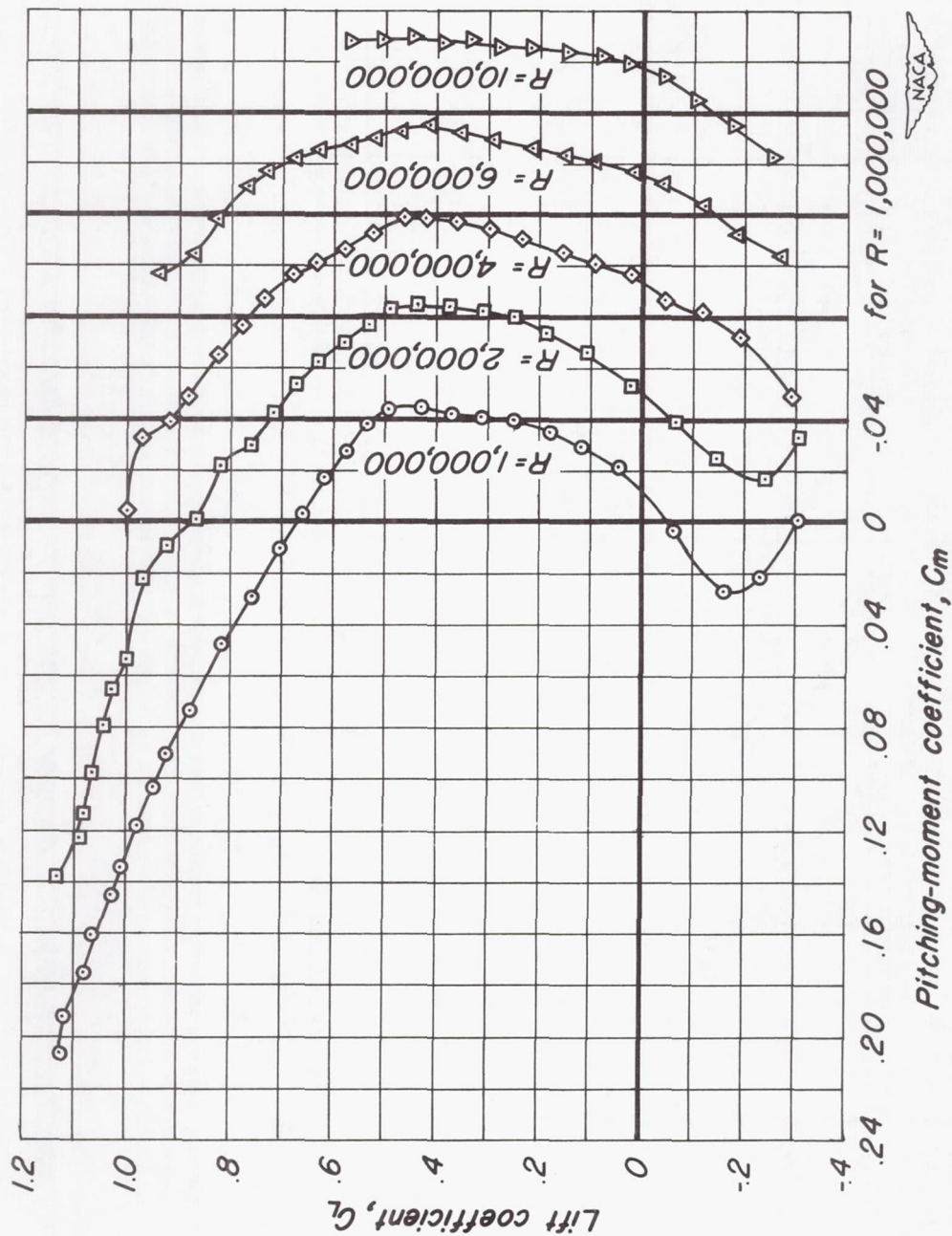
(c) C_L vs C_m

Figure 16.- Concluded.
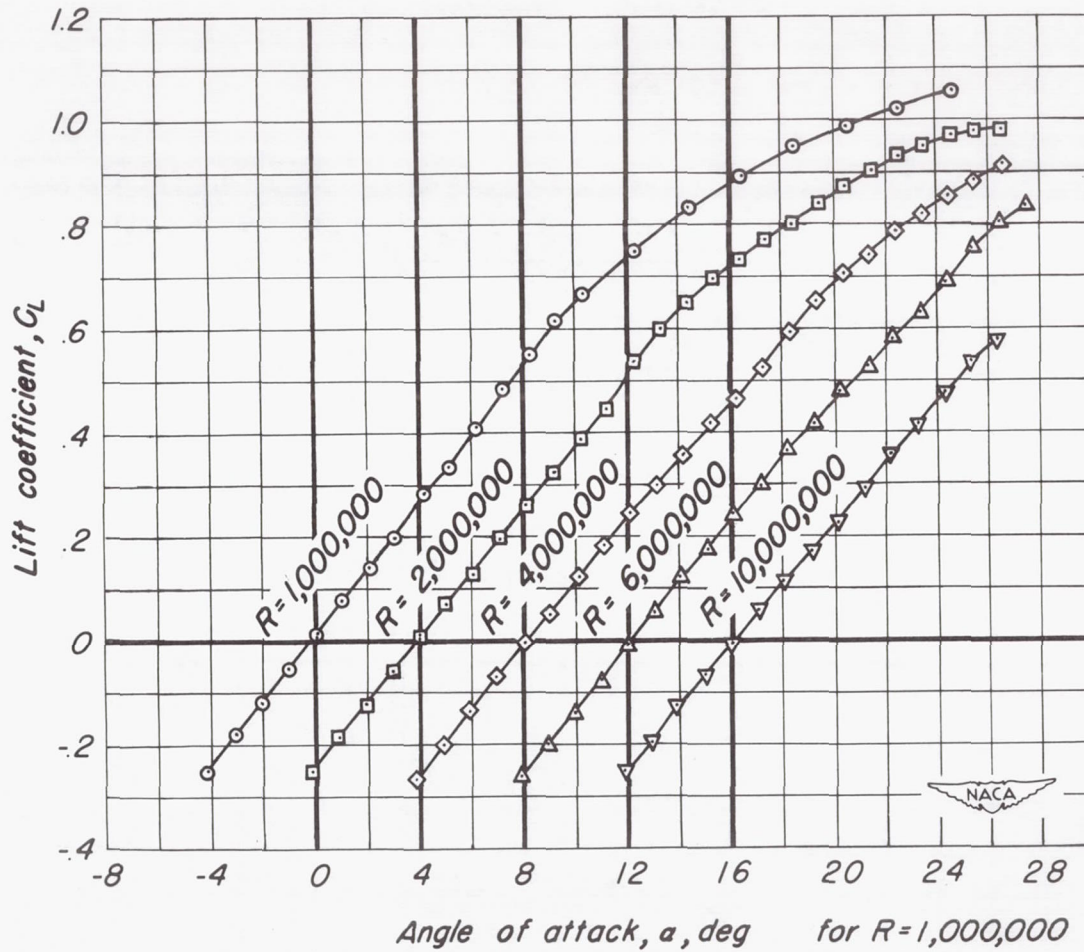
(a) C_L vs α

Figure 17. - The effect of Reynolds number on the aerodynamic characteristics of the full-span model with the plane wing at a Mach number of 0.25.
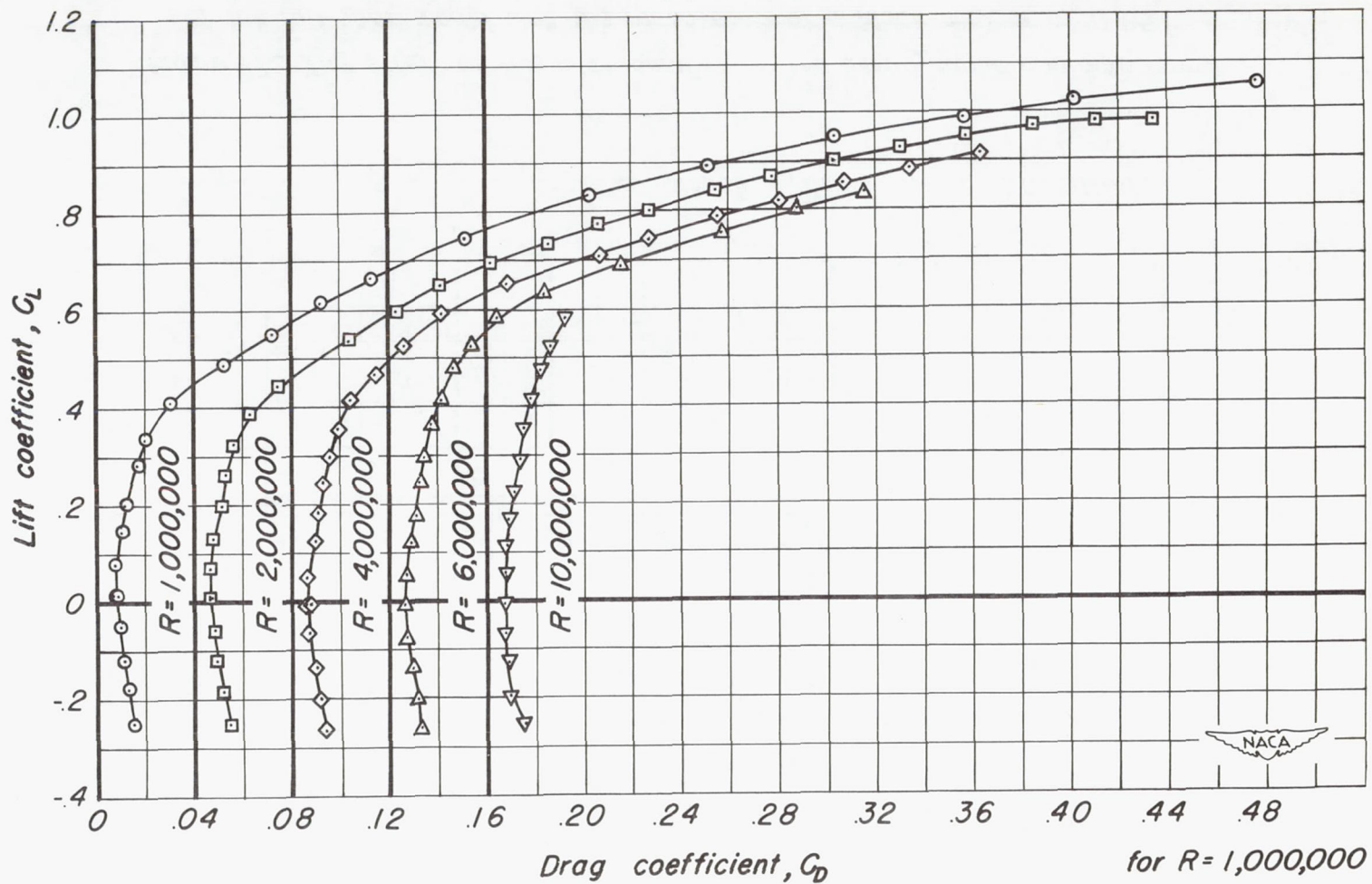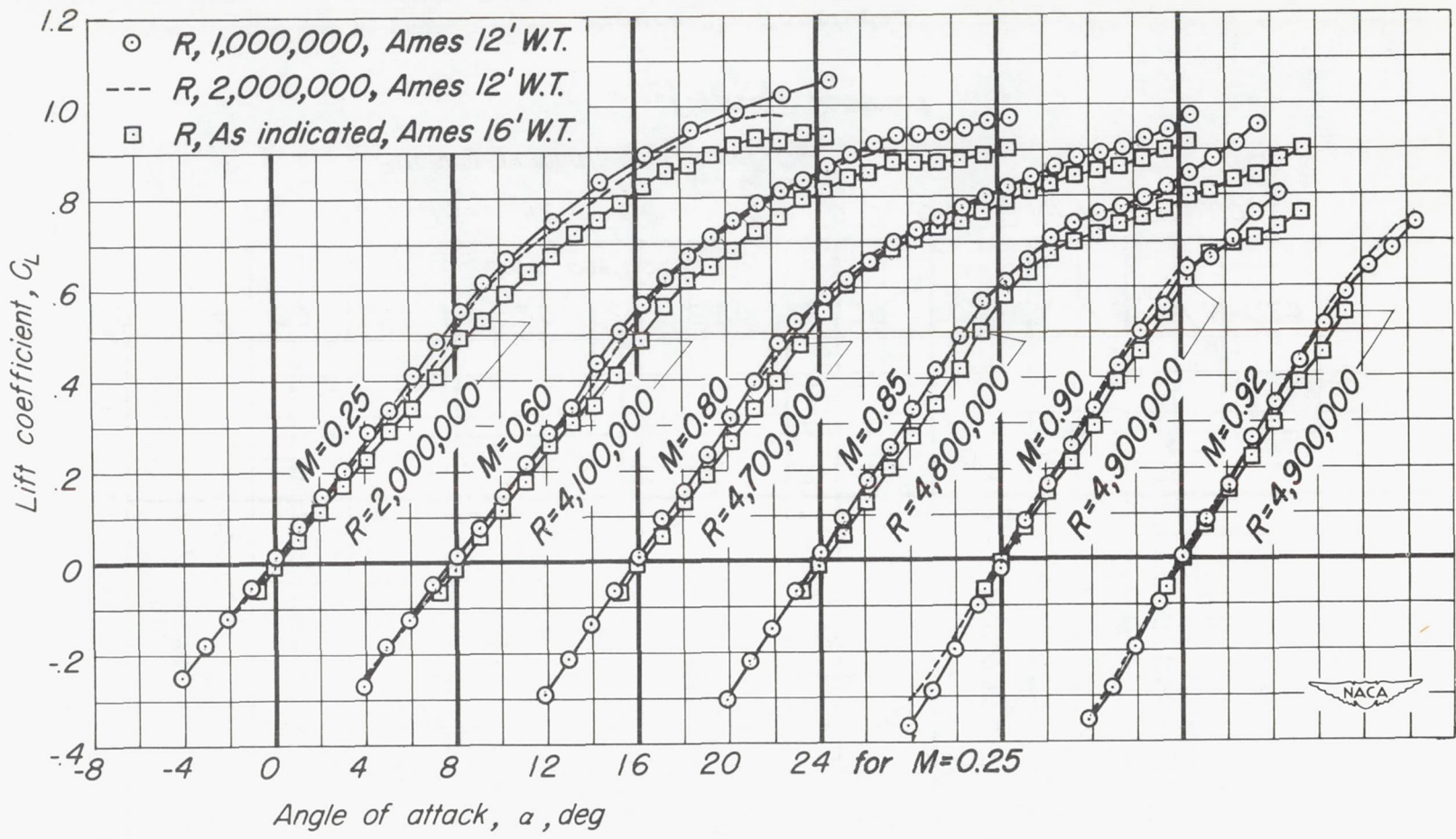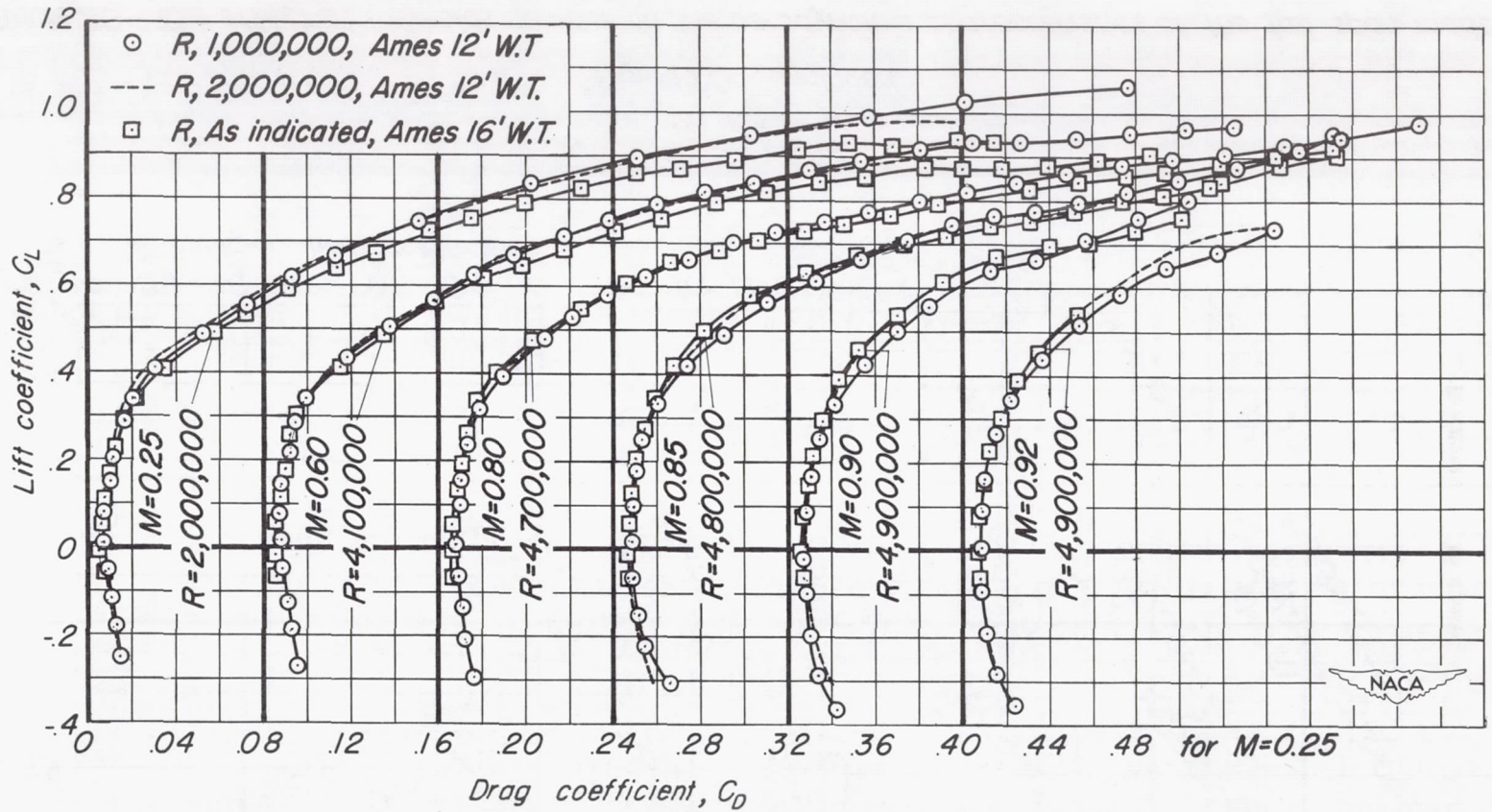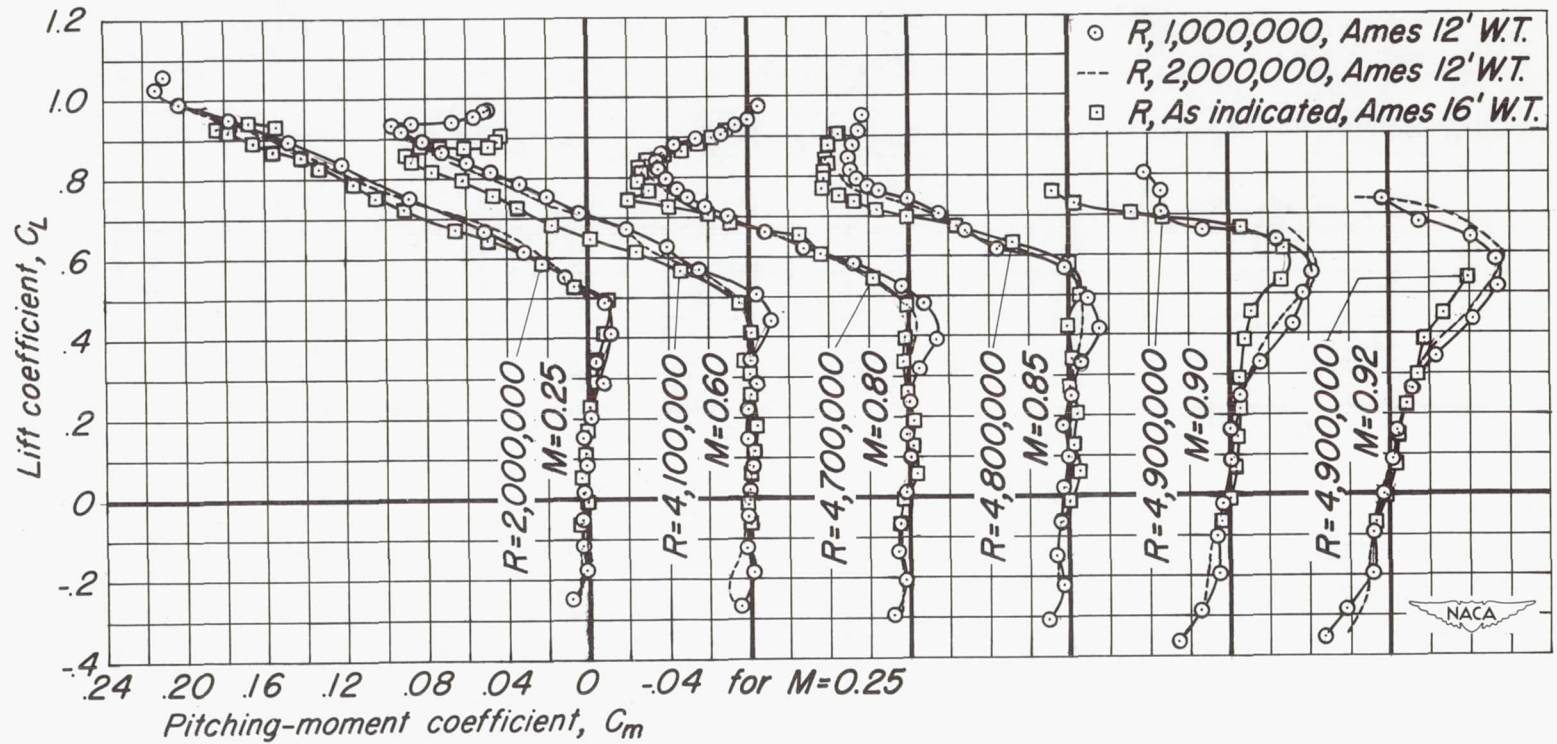
(b) C_L vs C_D

Figure 17.- Continued.

Pitching-moment coefficient, C_m
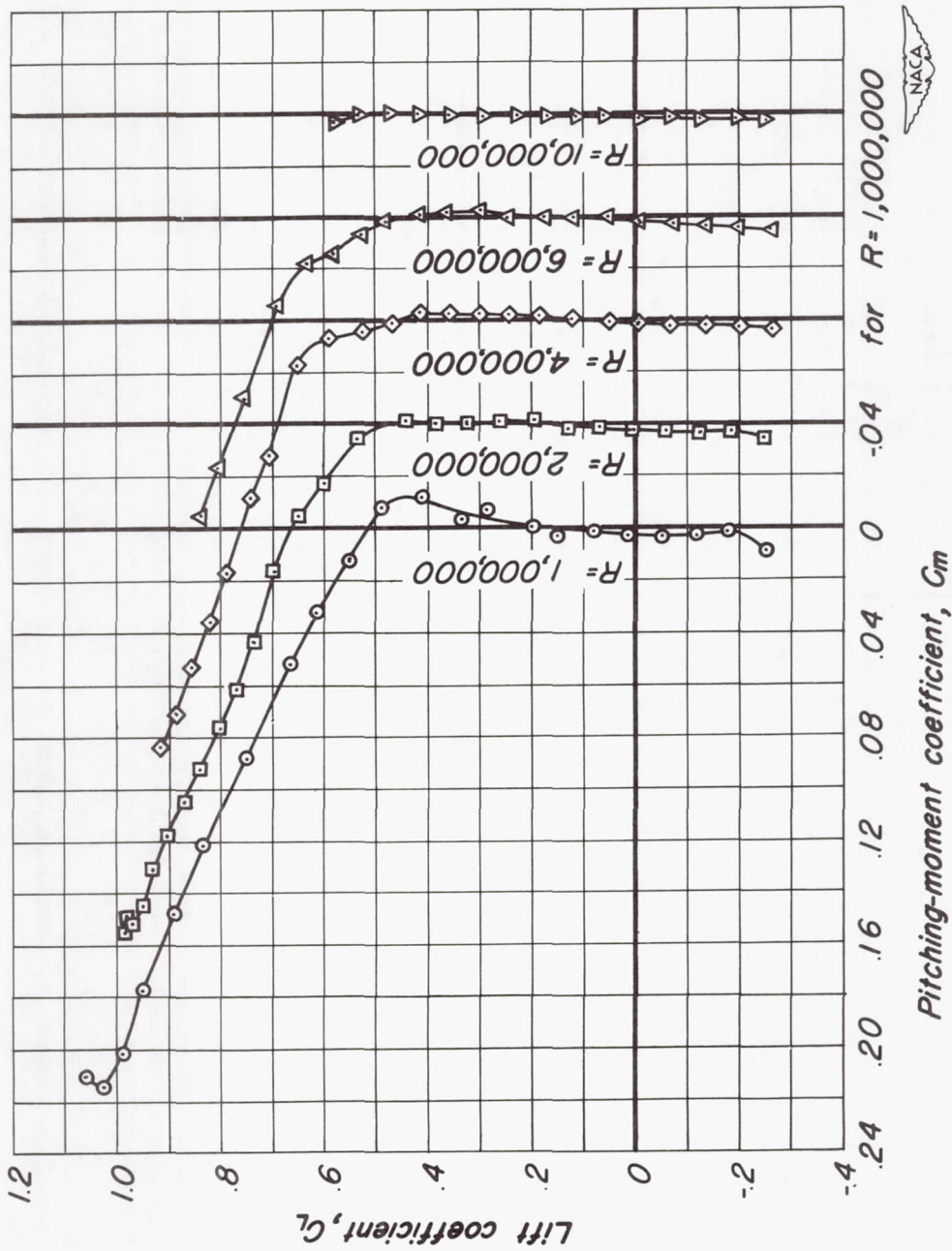
(c) C_L vs C_m

Figure 17.- Concluded.
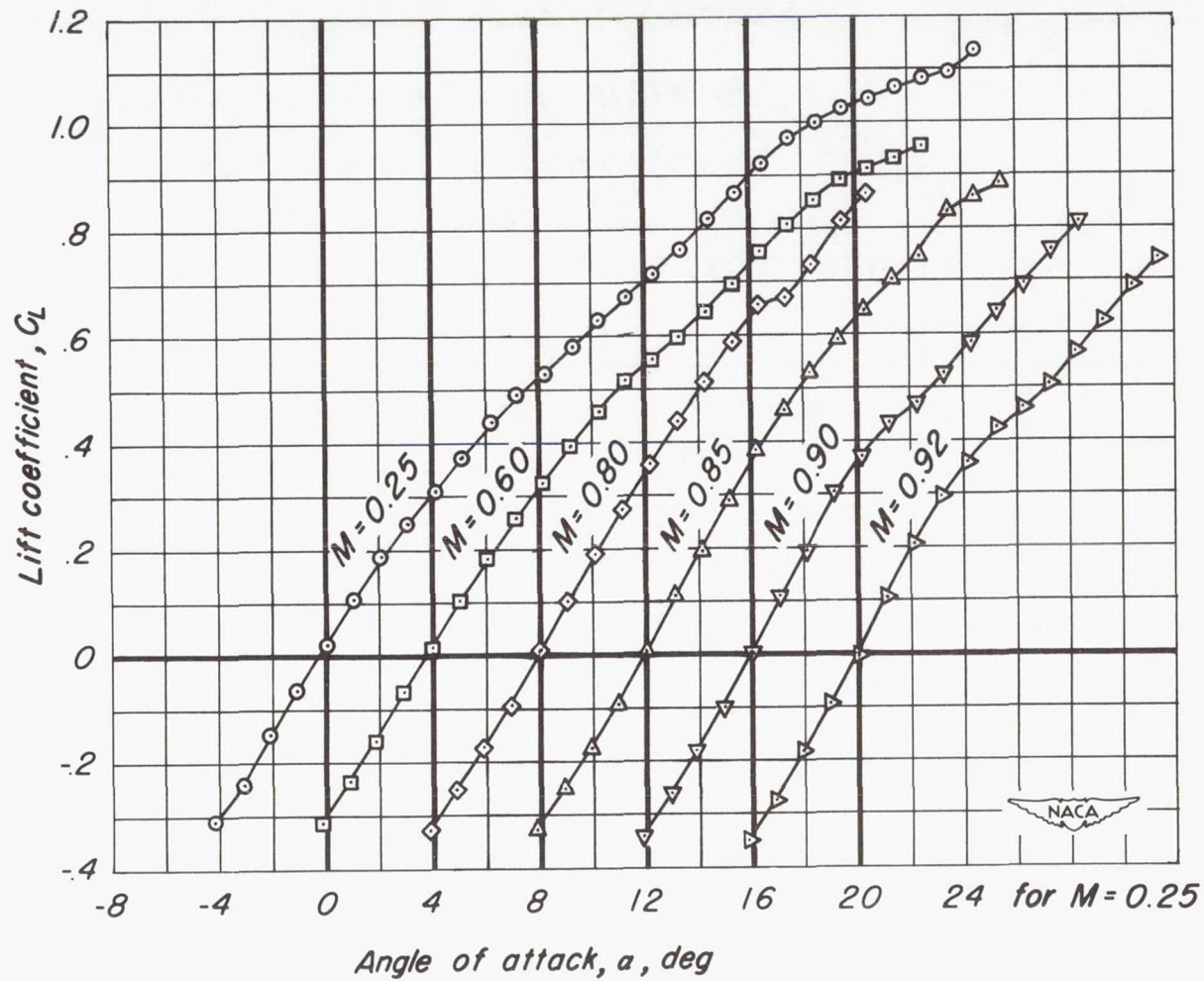
(a) C_L vs a

Figure 18.–The effect of Mach number on the aerodynamic characteristics of the full-span model with the cambered and twisted wing at a Reynolds number of 2,000,000.

Drag coefficient, C_D
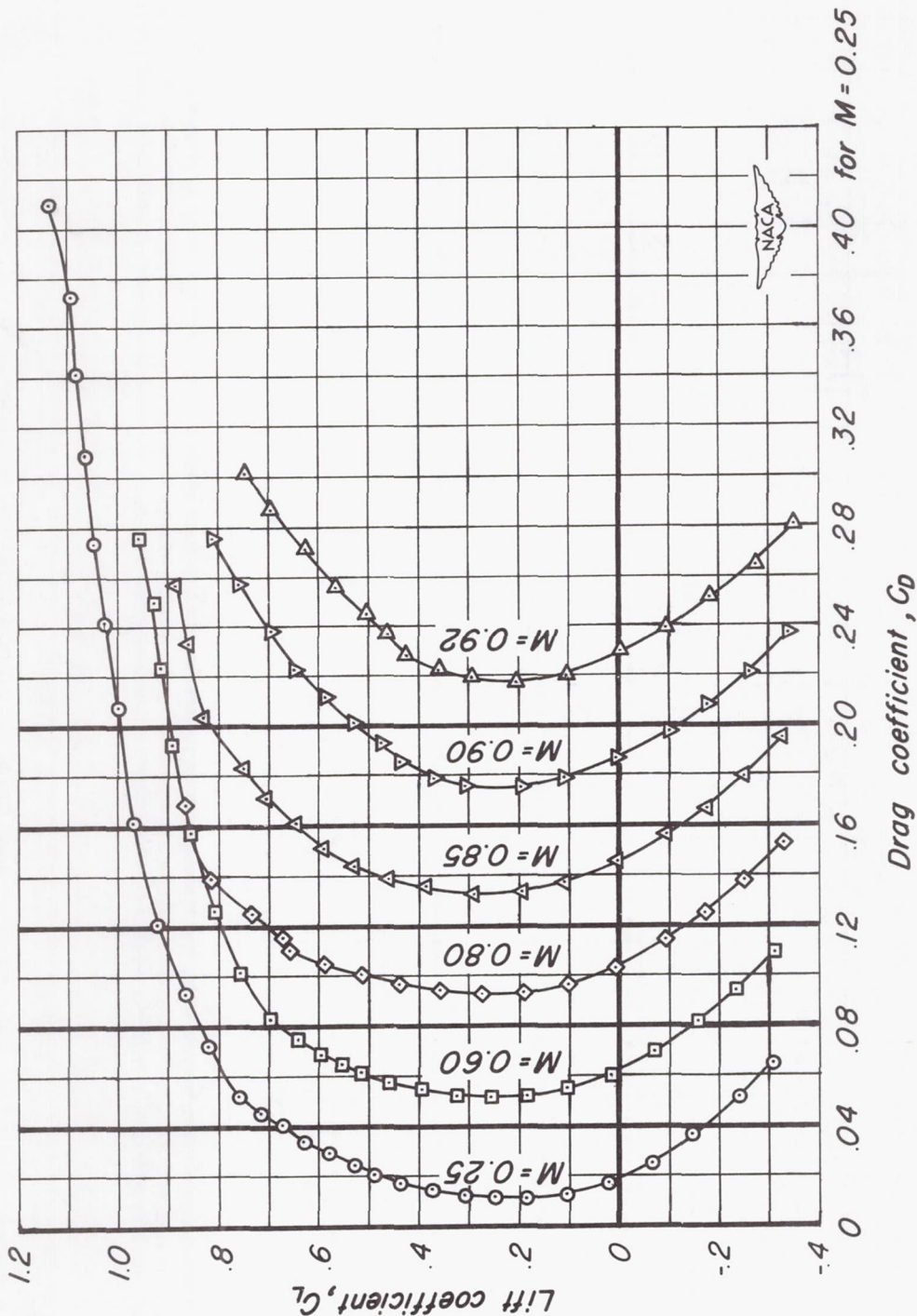
(b) C_L vs C_D

Figure 18.—Continued.
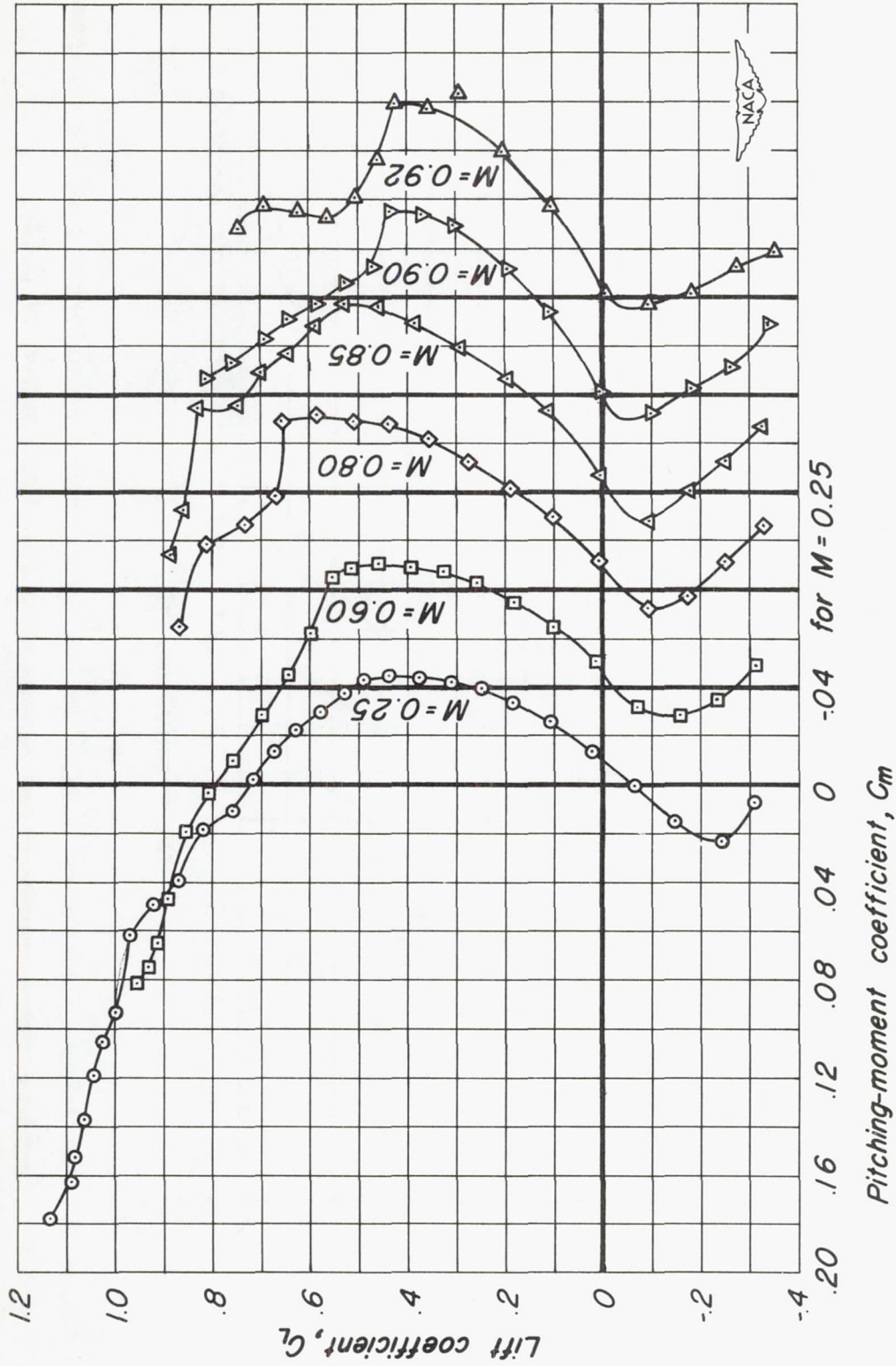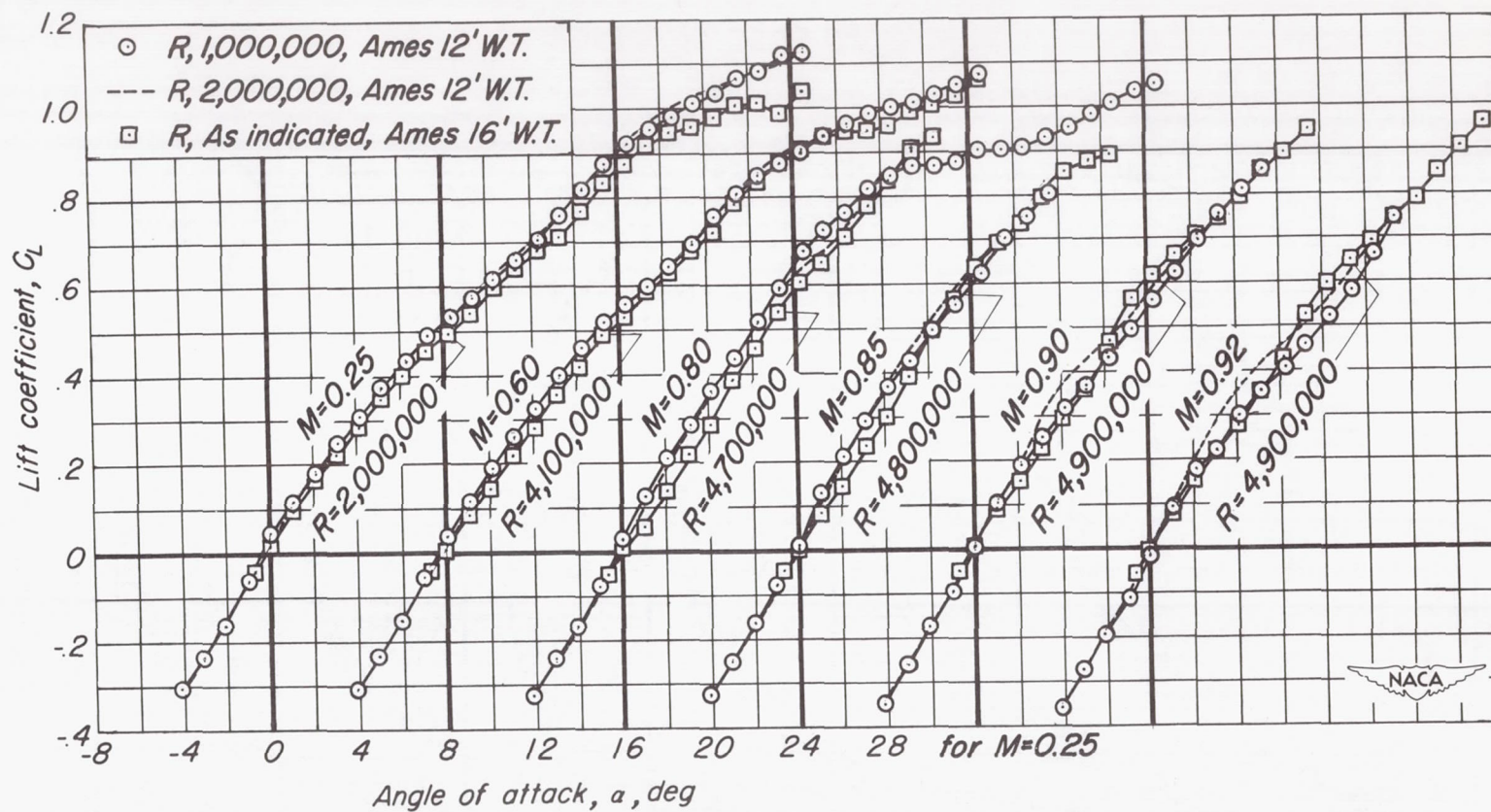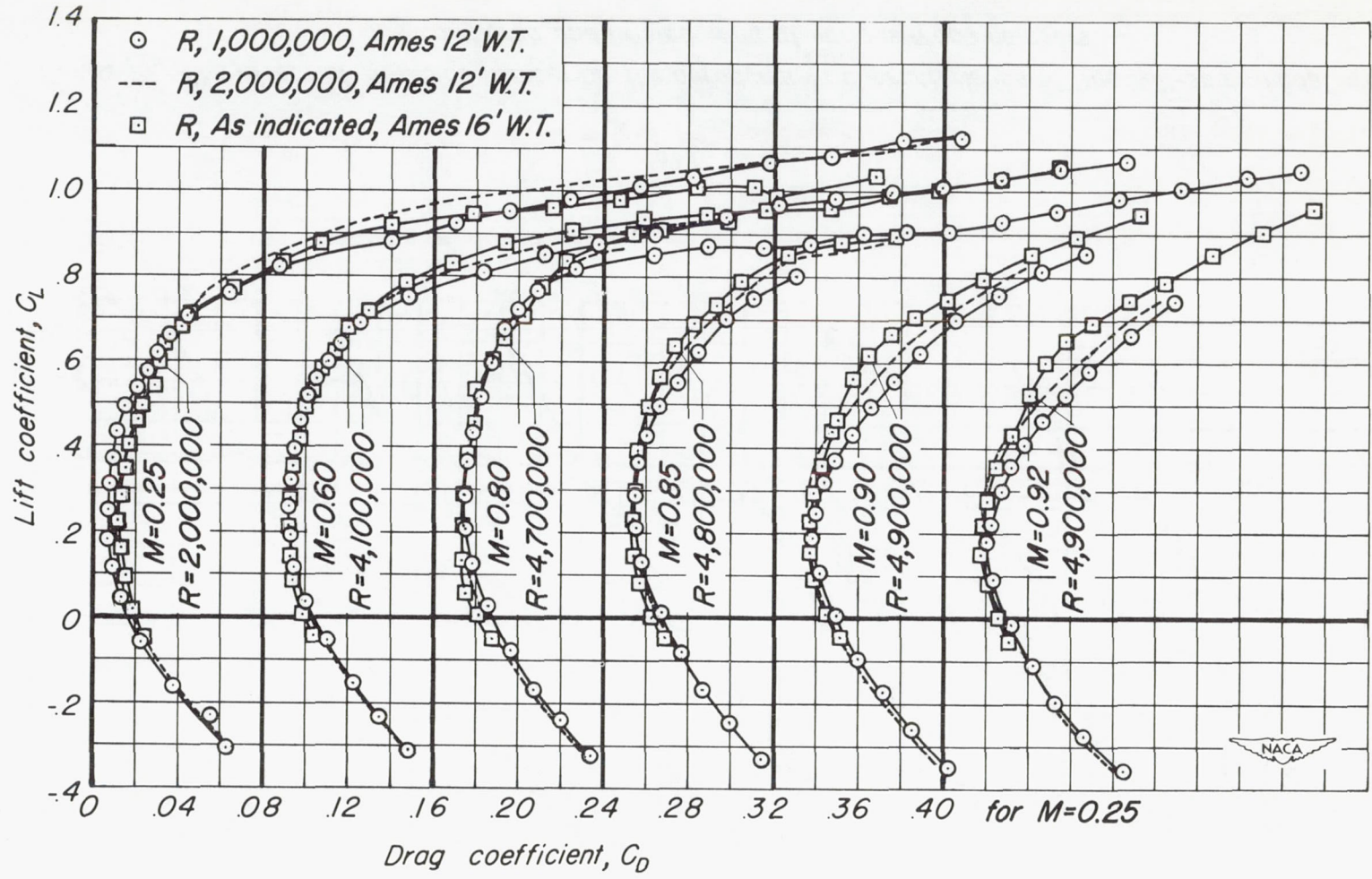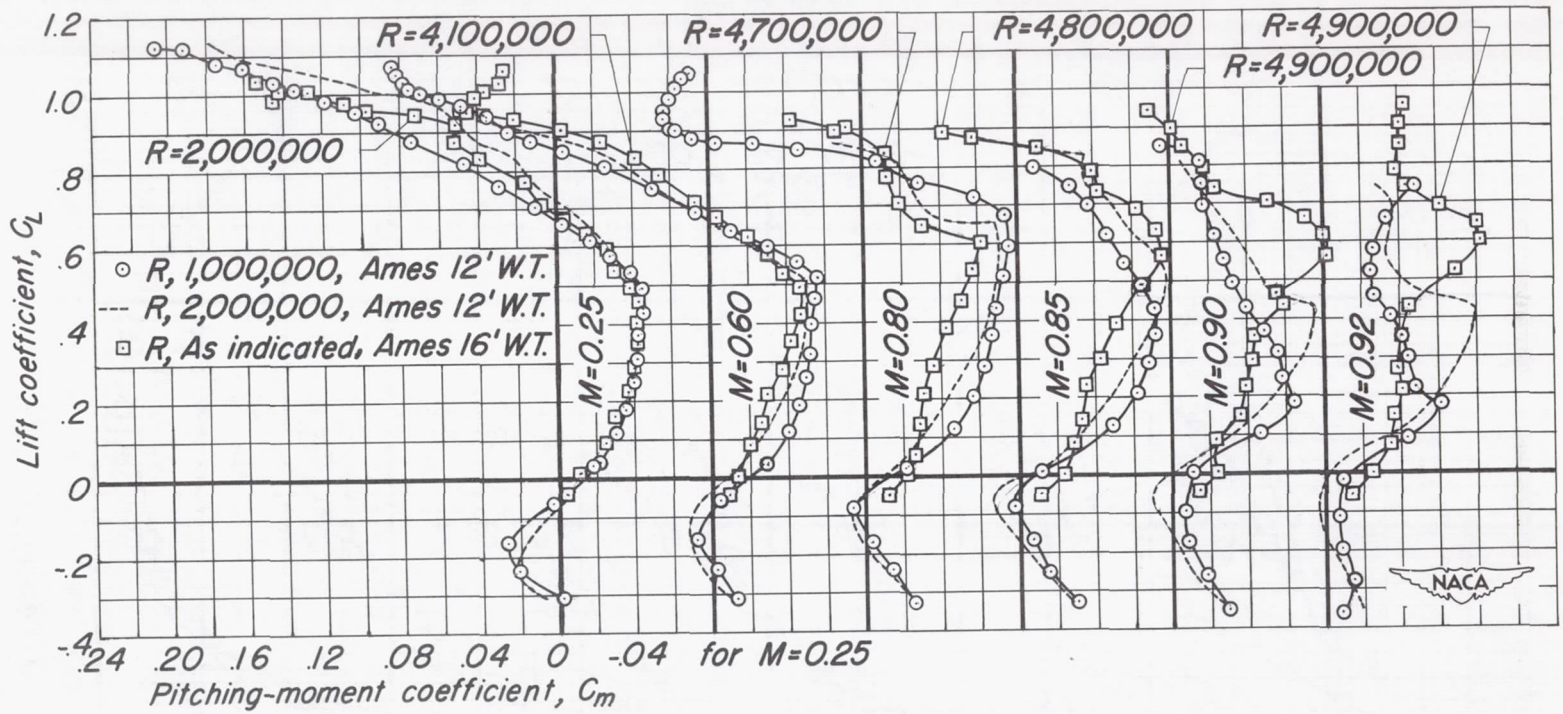
(c) C_L vs C_m

Figure 18.-Concluded.
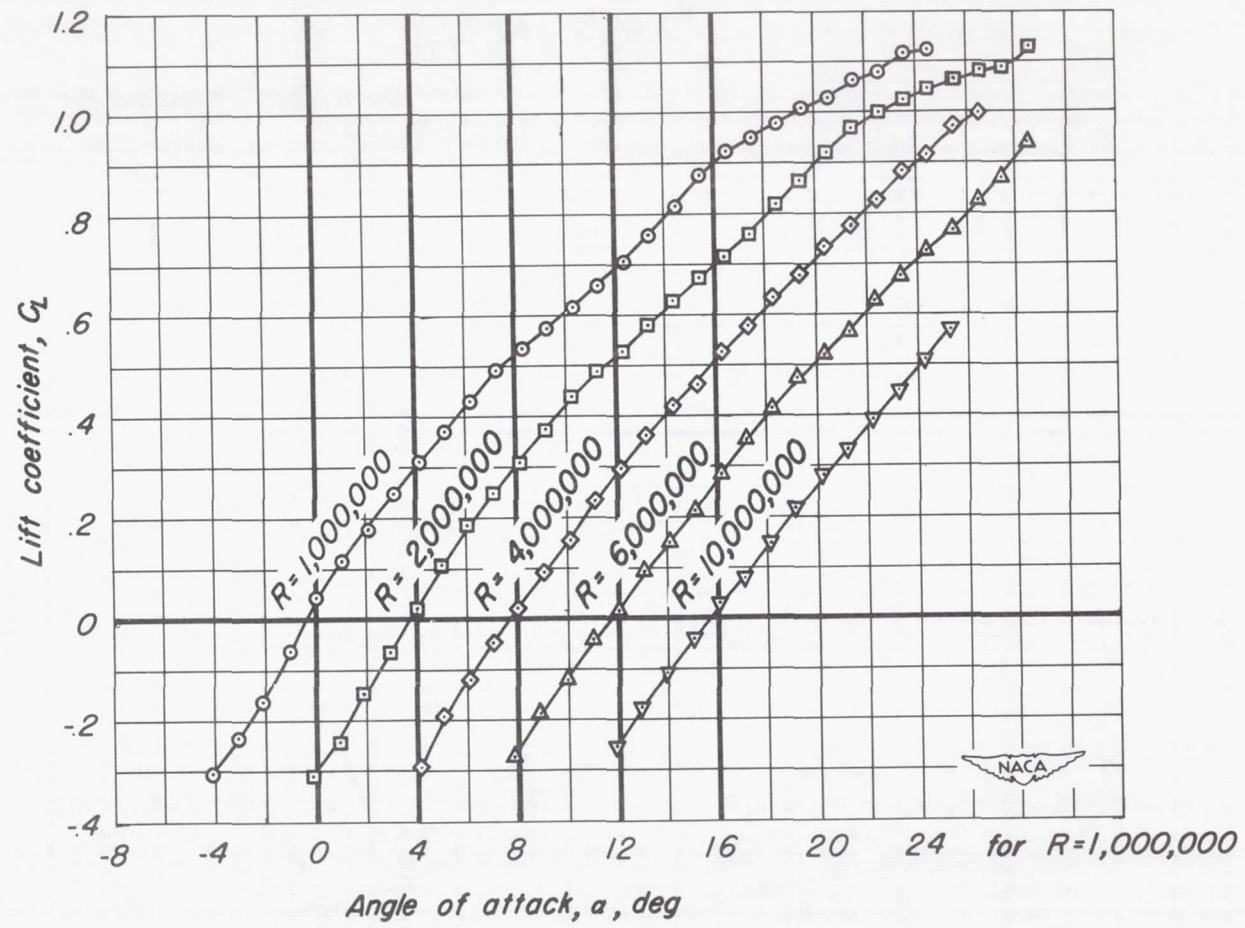
(a) C_L vs a

Figure 19.- The effect of Reynolds number on the aerodynamic characteristics of the full-span model with the cambered and twisted wing at a Mach number of 0.25.
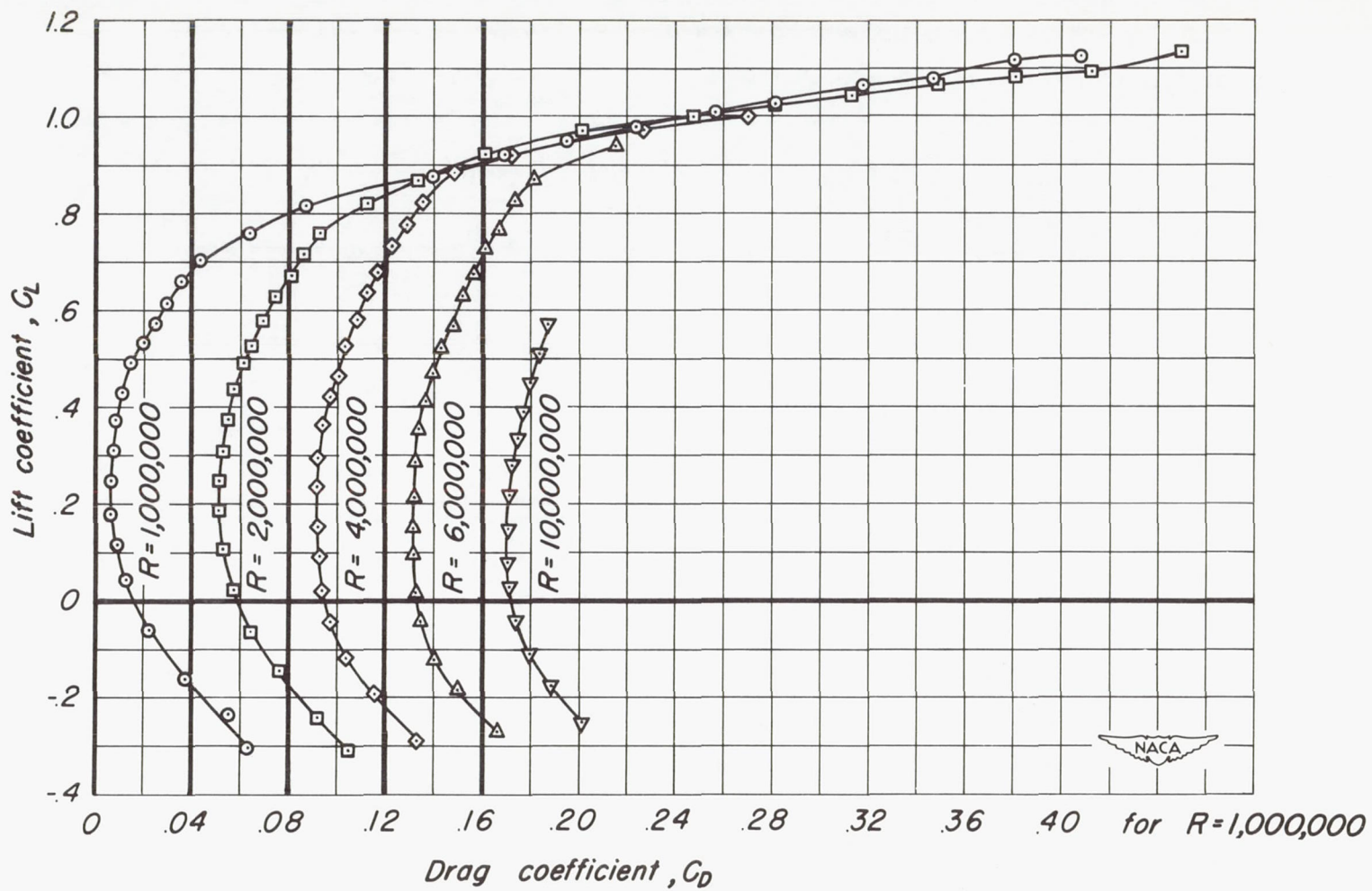
(b) C_L vs C_D

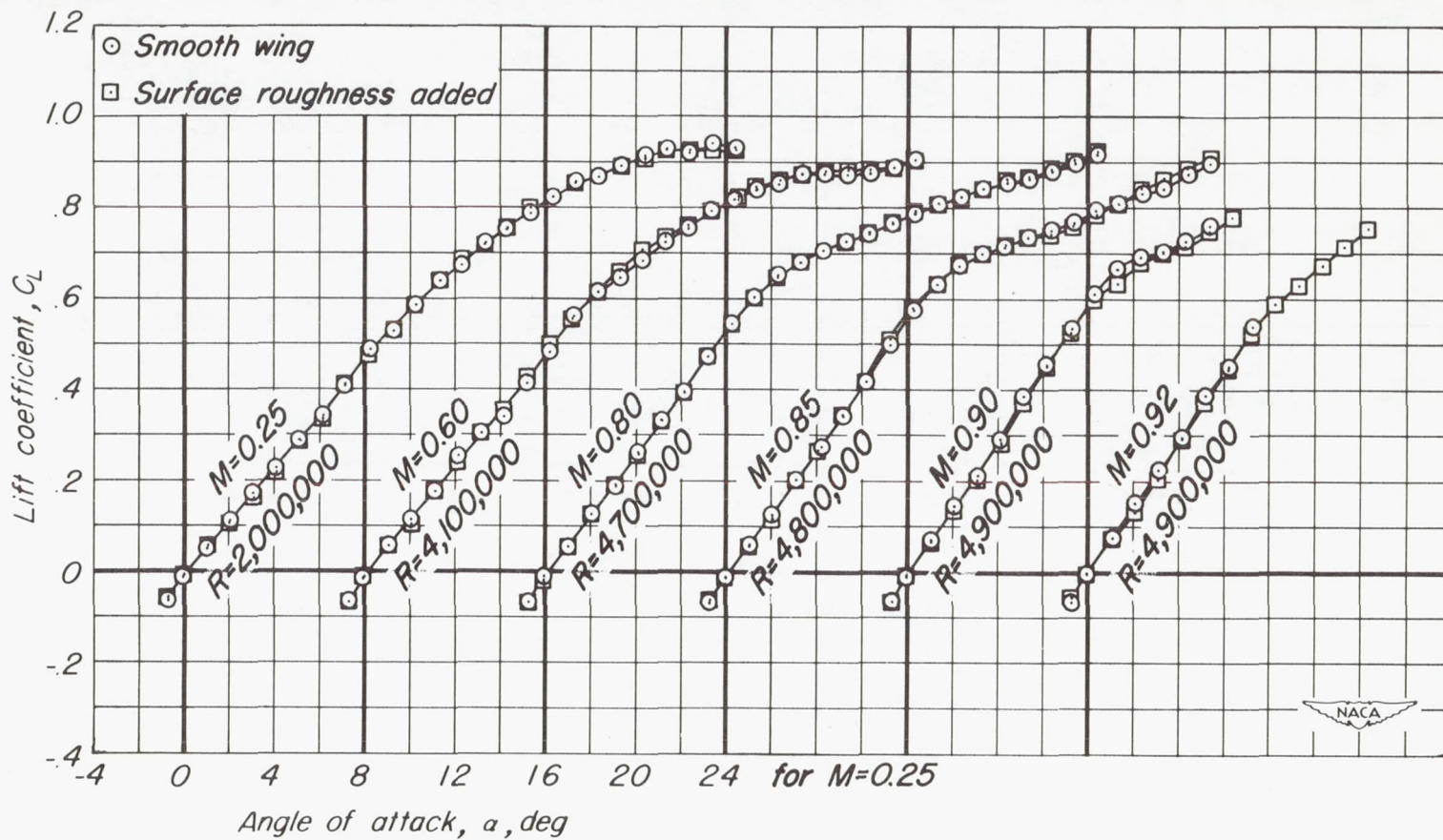Figure 19.- Continued.

(c) C_L vs C_m

Figure 19.- Concluded.

(a) C_L vs α

Figure 20.- The effect of Reynolds number on the aerodynamic characteristics of the full-span model with the plane wing at various Mach numbers.

Legend:
- ⊙ R, 1,000,000, Ames 12' W.T
- --- R, 2,000,000, Ames 12' W.T.
- □ R, As indicated, Ames 16' W.T.

M=0.25, R=2,000,000
M=0.60, R=4,100,000
M=0.80, R=4,700,000
M=0.85, R=4,800,000
M=0.90, R=4,900,000
M=0.92, R=4,900,000

Lift coefficient, C_L

Drag coefficient, C_D

for M=0.25

(b) C_L vs C_D

Figure 20.- Continued.

(c) C_L vs C_m

Figure 20.-Concluded.

(a) C_L vs a

Figure 21.- The effect of Reynolds number on the aerodynamic characteristics of the full-span model with the cambered and twisted wing at various Mach numbers.

(b) C_L vs C_D

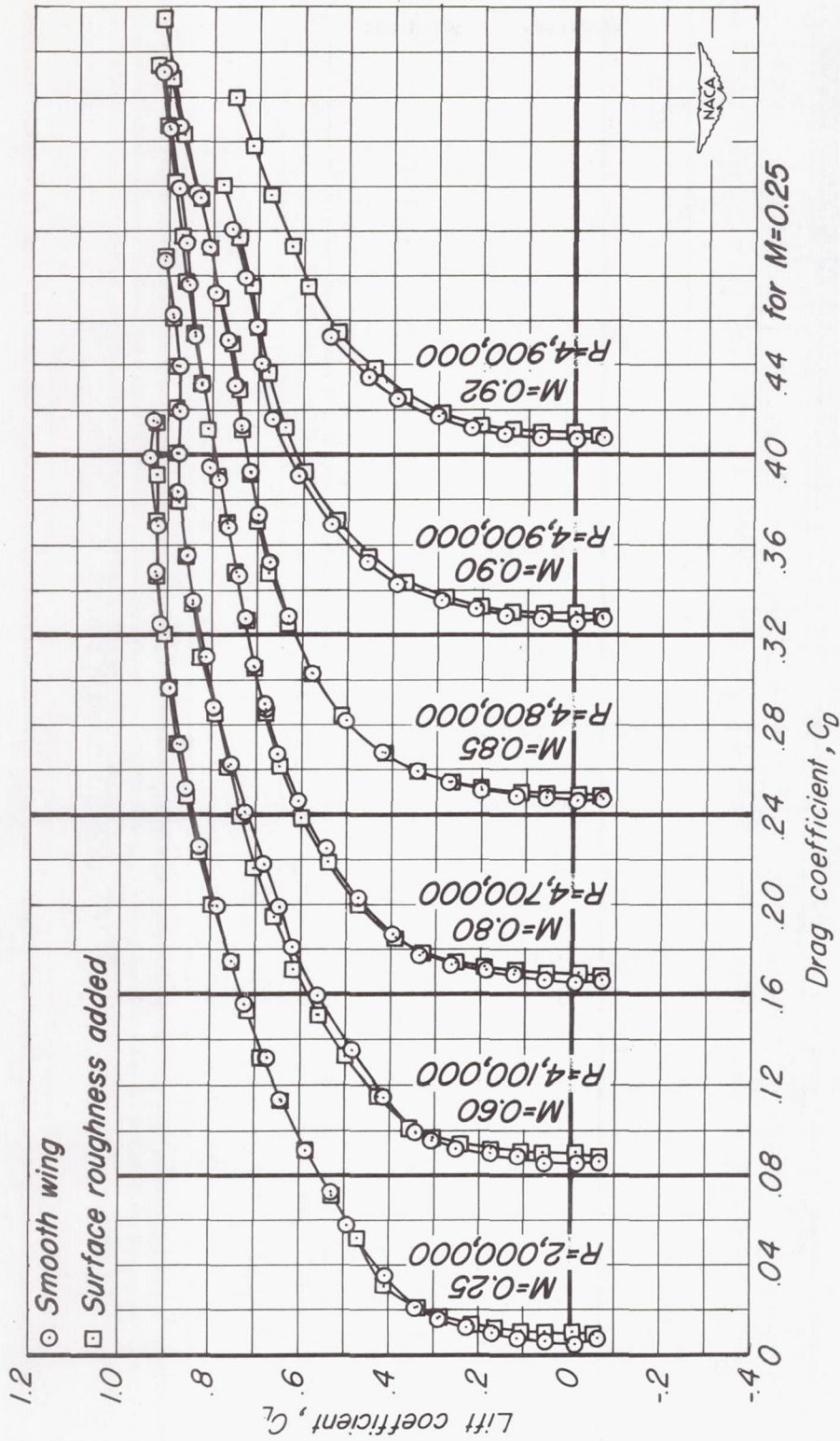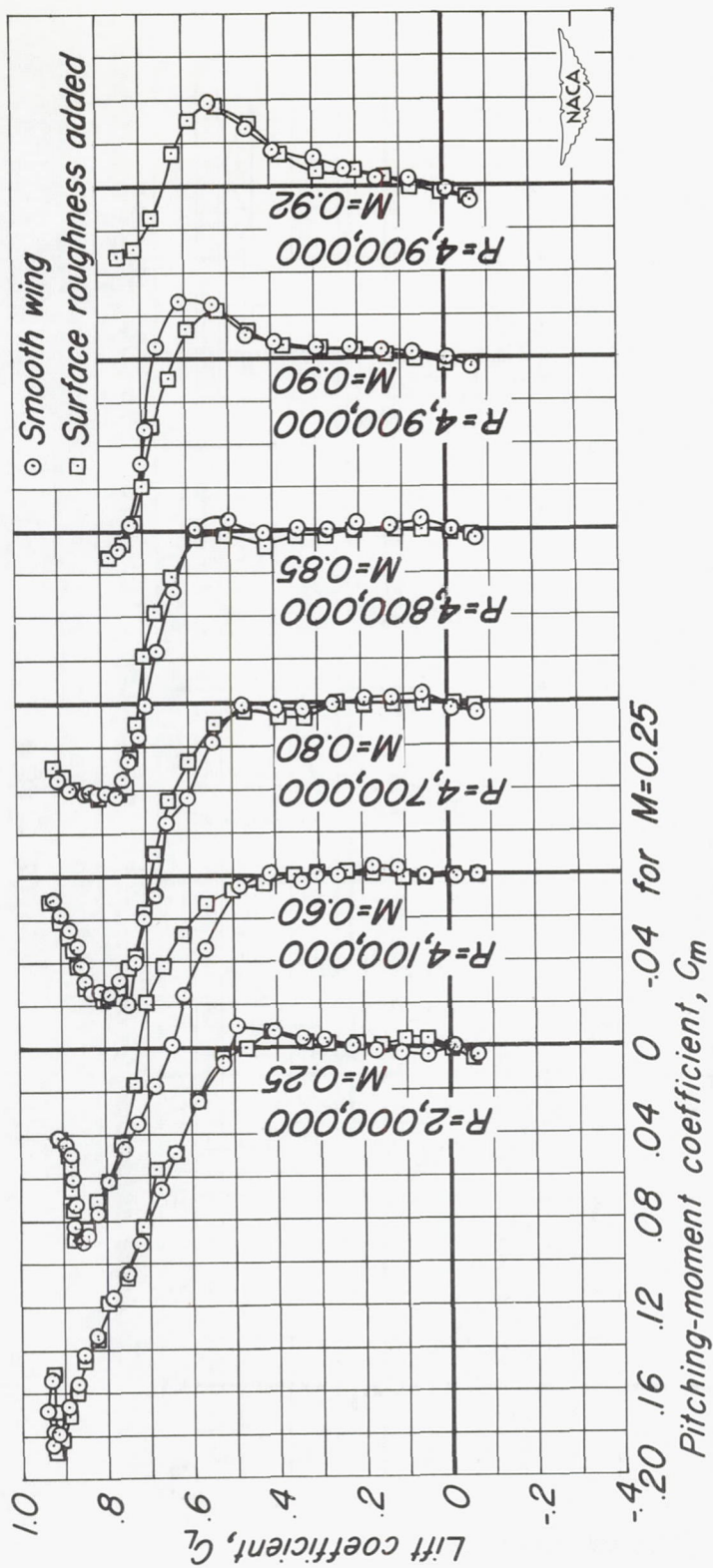*Figure 21.-Continued.*

(c) C_L vs C_m

Figure 21.- Concluded.

(a) C_L vs a

Figure 22.–The effect of surface roughness on the aerodynamic characteristics of the full-span model with the plane wing.
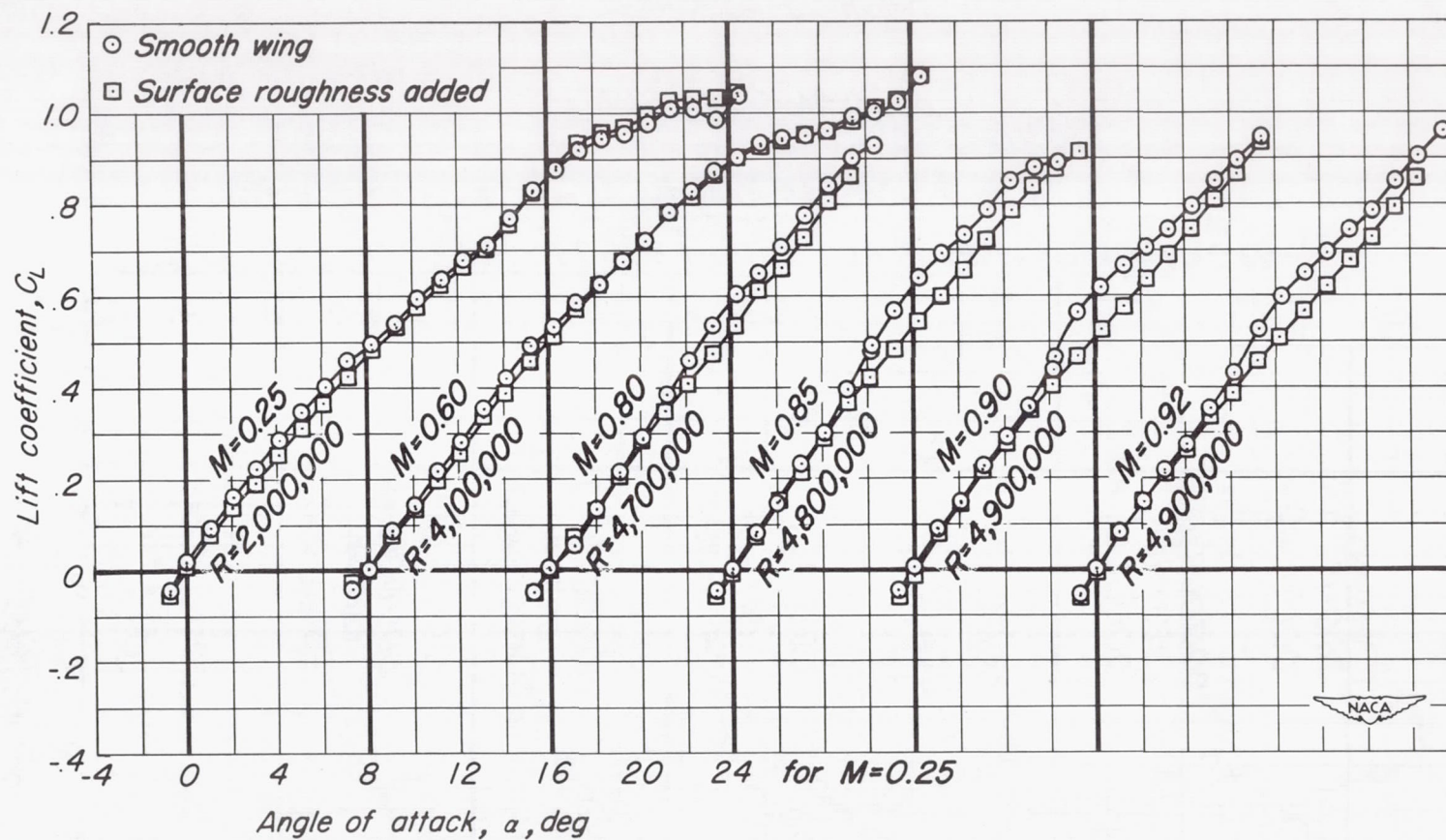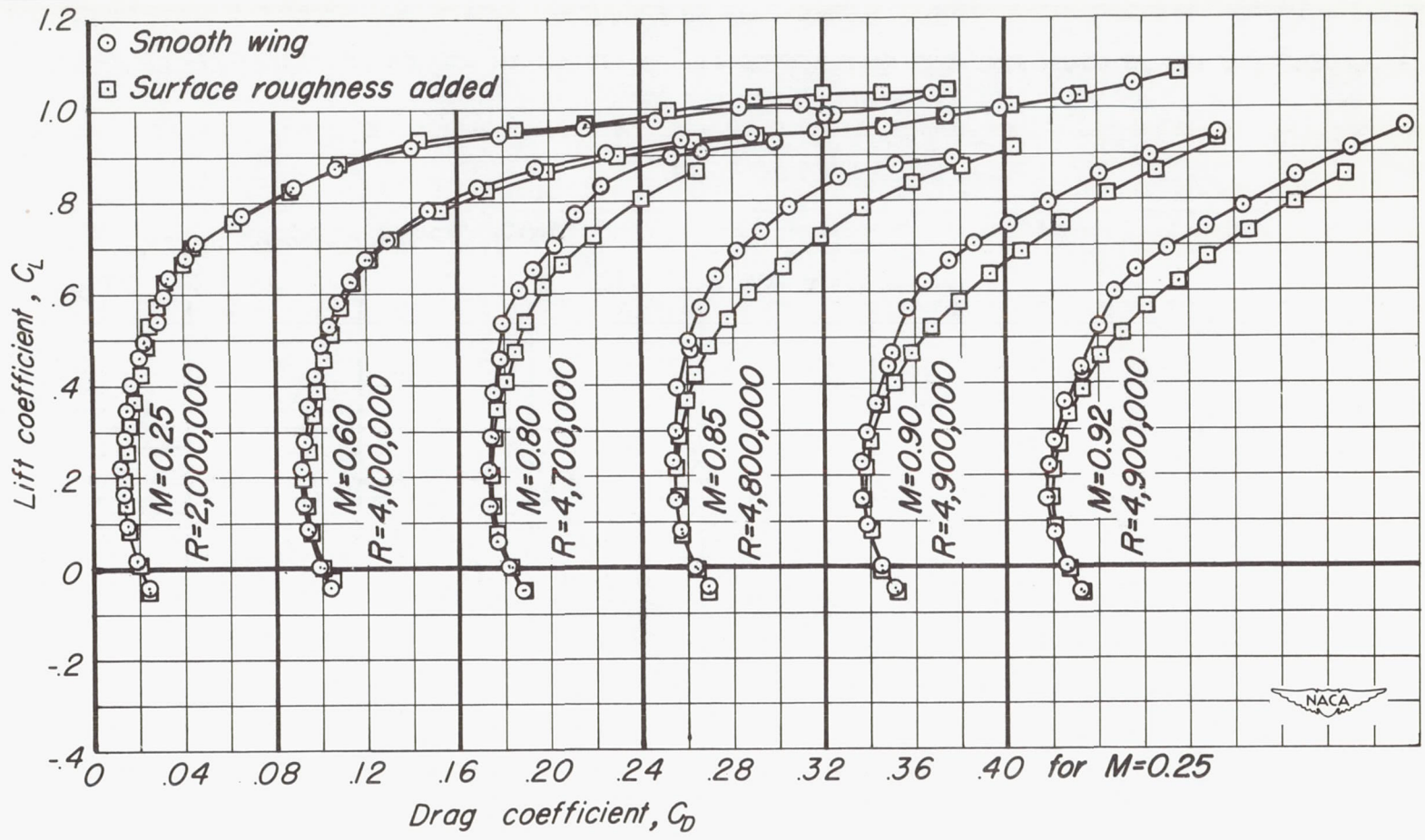
(b) C_L vs C_D

Figure 22.-Continued.
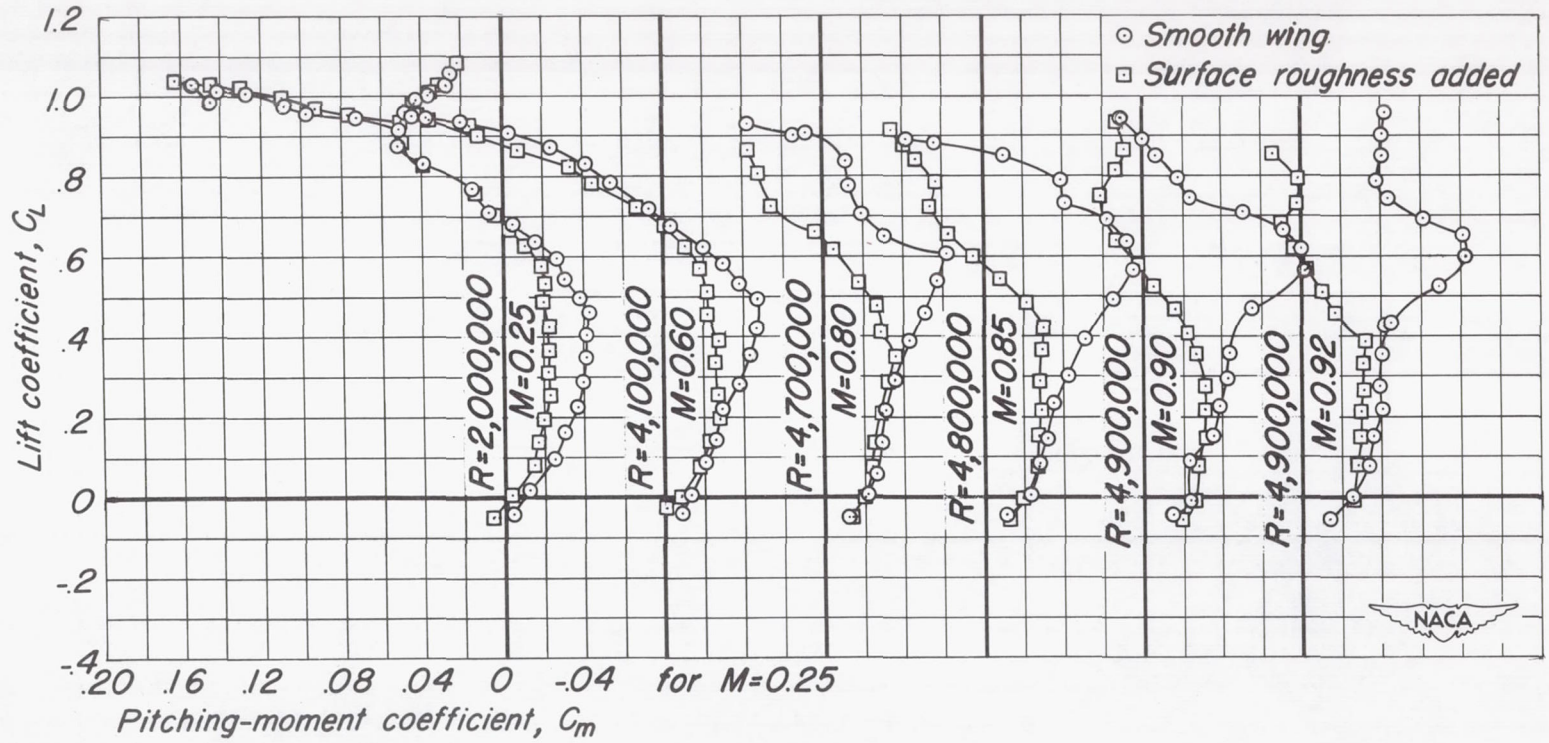
(c) C_L vs C_m

Figure 22.- Concluded.

(a) C_L vs a

Figure 23.–The effect of surface roughness on the aerodynamic characteristics of the full-span model with the cambered and twisted wing.

(b) C_L vs C_D

Figure 23.-Continued.

(c) C_L vs C_m

Figure 23.- Concluded.